CHAPTER 1

Sketches of the Standard Imaging Modalities

Different Ways of Creating Visible Contrast Among Tissues

The principal job of a medical imaging modality is to provide clear maps of anatomy, or to make it possible to identify irregularities in physiology, or both (Figure 1.1). It does so by creating contrast among tissues, and the various modalities do this in biophysically diverse ways.

This chapter provides brief sketches of the major imaging technologies that are employed routinely in modern diagnostic clinics to examine the structure and functioning of the body. It begins with modalities slowly developed over the first three quarters of the twentieth century, like screen-film

Medical Imaging: Essentials for Physicians, First Edition. Anthony B. Wolbarst, Patrizio Capasso and Andrew R. Wyant.

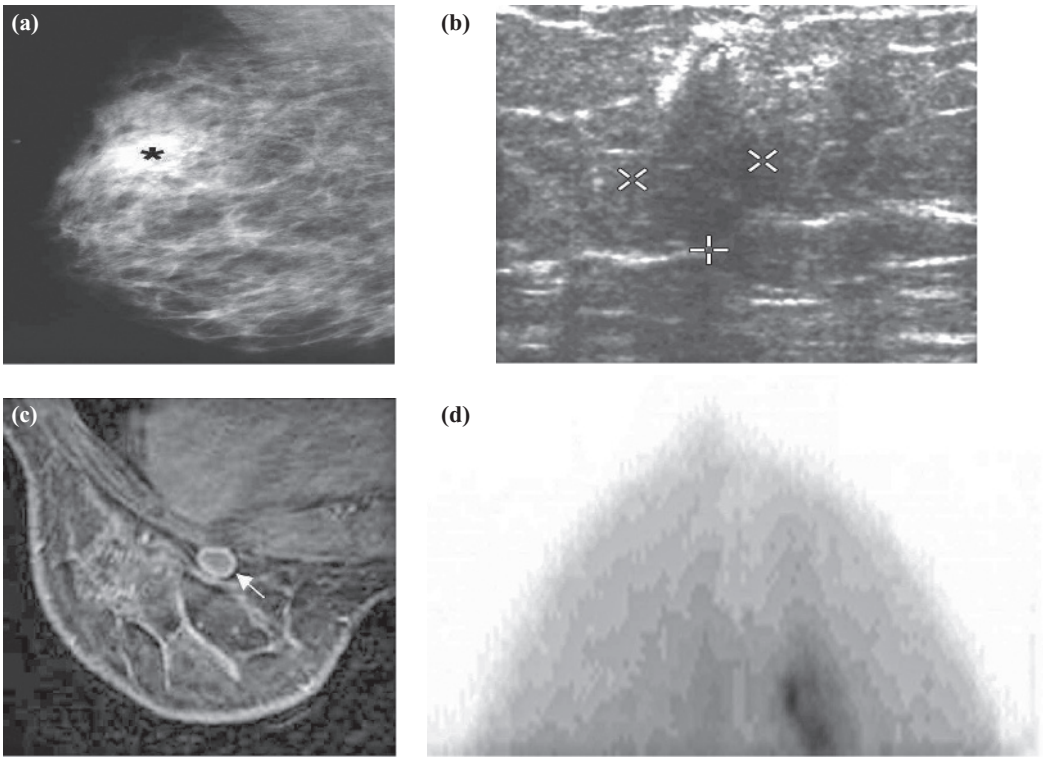

Figure 1.1 Breast imaging for a patient with a biopsy-proven lobular carcinoma. **(a)** When a woman has her routine annual digital mammographic examination after the age of 40, two nearly orthogonal views are obtained of each breast. Mammography demands high soft-tissue contrast to detect neoplasms and fine resolution to examine microcalcifications but, at the same time, very low dose deposition. **(b)** B-mode ultrasound is often able to distinguish quickly, reliably, and inexpensively between a fluid-filled cyst and a solid tumor detected earlier with mammography. Here, the acoustic attenuation confirms the presence of a suspicious solid lesion. **(c)** MRI is often the screening tool of choice for patients at high risk for breast cancer. **(d)** PET with its standard radiopharmaceutical fluorine-18 deoxyglucose (^{18}FDG) is highly sensitive to tissues that, like many tumors, consume an excessive amount of glucose. These modalities produce contrast through radically different biophysical mechanisms, and provide complementary kinds of medical information.

radiography and mammography, image-intensifier tube fluoroscopy, and analog nuclear medicine (NM) and ultrasound (US) imaging. Then came twenty-first century technologies that have flourished only with the advent of high-speed and powerful, but small and affordable, computers – digital planar imaging like computed radiography (CR); digital radiography (DR); digital mammography (DM); digital fluoroscopy (DF), including digital subtraction angiography (DSA); computed tomography (CT), culminating in helical, multi-detector ring CT (MDCT); single photon emission computed tomography (SPECT) and positron emission tomography (PET); advanced forms of B-mode and Doppler US; and magnetic resonance imaging (MRI) in all its glory, with T1-, T2-, and proton density-weighted imaging, functional MRI (*f*MRI), MR angiography (MRA), diffusion tensor imaging (DTI), and many other variants. All of these modalities will be discussed further in the forthcoming chapters.

"Roentgen has surely gone crazy!"

Although no one realized it at the time, the discovery of X-rays in 1895 foreshadowed the quantum upheavals that would turn the physical sciences upside down in the first quarter of the twentieth century. More immediately and spectacularly, however, it flung open a door that led into a new and

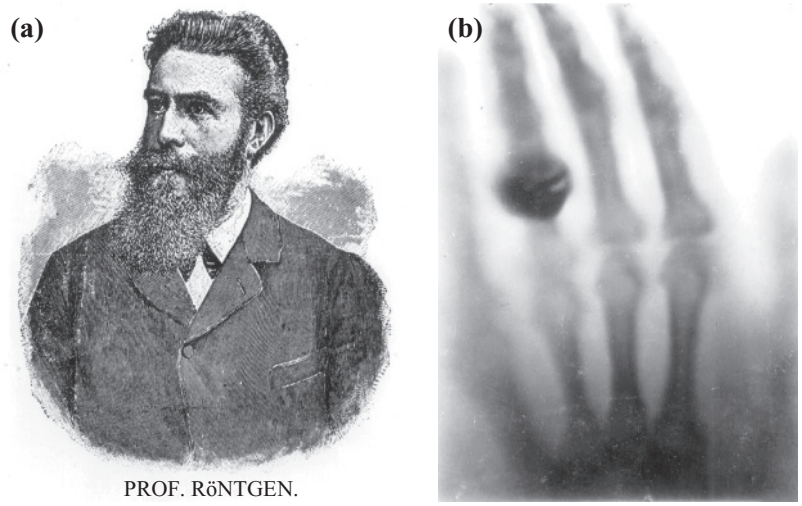

Figure 1.2 In the beginning ... **(a)** An engraving of Wilhelm Conrad Roentgen, from *Something About X-rays for Everyone*, which was published in 1896, less than a year after his discovery. Reproduced from Trevert E, *Something about X-rays for Everyone*, 1896. Reprinted by Medical Physics Publishing Company, Madison, WI, 1988. Soon thereafter, one visitor described him as "a very tall man, with a scholarly stoop, his face somewhat pockmarked, stern but kindly, and very modest in his remarks upon his achievements" (Mould RE, *A Century of X-Rays and Radioactivity in Medicine*, Institute of Physics Publishing, London, 1993). **(b)** The earliest extant X-ray record, of Roentgen's wife Bertha's hand and signet ring, taken by her husband on December 22, 1895. Courtesy of the Deutsches Roentgen-Museum, Remscheid-Lennep, Germany.

completely unanticipated dimension in the practice of medicine — the ability to look non-invasively within a patient's body, without having to cut into it.

A century ago, medical diagnosis was as much art as science. The doctor could measure body temperature, blood pressure, pulse rate, and a few simple chemical attributes of blood and urine, but not much else. Odors and subtle aspects of a patient's appearance during a physical examination often provided equally important clues. But medicine lacked any means to view the interior of the body directly, apart from surgery, to reach critically important diagnoses.

That abiding problem ceased to exist, literally overnight, on the evening of November 8, 1895, when the German physicist Wilhelm Conrad Roentgen chanced upon X-rays (Figure 1.2a). Roentgen, a respectable but little known professor at the University of Würzburg, had been experimenting with an apparatus of widespread scientific interest at the time that is now called a *cathode ray tube* – a partially evacuated glass tube containing two metal electrodes at its opposite ends that were attached to the outside world by means of a pair of wires passing through the glass. Scientists had been intrigued by what happens when a high voltage is applied between the electrodes: the thin gas within would glow, as would the glass itself in the area near the anode (the electrode attached to the positive pole of the voltage source). It was argued that the agent responsible for this phenomenon was some sort of wave or particle, perhaps negatively charged, that emerged from the cathode (the negative electrode) and that was attracted toward the anode. These so-called "cathode rays" presumably excited the gas and, on striking glass, caused it to fluoresce as well. The nature of cathode rays themselves, now understood to be ordinary electrons, remained obscure for several more years after Roentgen's discovery.

It is not clear what Roentgen was attempting on November 8, since his will stipulated that all of his laboratory notes be burned unread upon his death. In any case, as he worked in a darkened room late in the evening, something unusual caught his eye: when an electric discharge occurred in his tube, a nearby piece of paper that happened to be coated with a chemical compound of barium, platinum,

and cyanide produced a glow. With his glass tube completely enveloped in black cardboard, there was no way that visible light from the tube could be reaching the coated paper. So something invisible had to be passing through the cardboard and reaching the barium platinum cyanide, inducing it to give off light. Roentgen had, in fact, discovered X-ray radiation by observing X-ray fluorescence (the emission of light caused by an X-ray stimulus) in a nearby material that was fluorescent. (Patton [1–3] provides a fascinating and detailed accounting of Roentgen's discovery.)

Roentgen was aware that he might have stumbled onto something altogether new, and he was excited and shaken by the remarkable thing he was seeing. But as he explored this totally unexpected phenomenon, he worried that perhaps there might be a simple, obvious explanation that he was overlooking. Far more disturbing was the possibility that perhaps he could not trust his own senses – after all, this appeared to be a physical process that was trivially easy to produce, and undeniably of extraordinary significance, so why had no-one else already seen it and reported it? He knew the physics literature well, and was quite certain that nothing like this had been described before. But were his observations genuine, or might they possibly be the creation of his own mind?

"I believed," he later recalled, "that I was the victim of deception when I observed the phenomenon of the ray" [4]. He wrote to his longtime friend, physicist Ludwig Zehnder: "I had spoken to no one about my work. To my wife I merely mentioned that I was working on something about which people would say, when they found out about it, 'Roentgen has surely gone crazy.'"

But Roentgen persevered. Placing various objects between the tube and the fluorescent screen, he learned that they affected the brightness of the emitted light by different amounts. A few pieces of paper or cardboard had little impact, but a thick sheet of metal quenched the light completely. And when he held his hand in the path of the beam, he could make out the bones of his fingers projected in silhouette upon the screen. A short while later, Roentgen produced the first X-ray record, permanently capturing his wife Bertha's hand and signet ring on a glass photographic plate (Figure 1.2b). Bertha, regrettably, was not overly impressed by the medical significance of the discovery – she had long harbored a terrifying premonition of an early death, and seeing the resemblance of her hand to a skeleton gave her a most unpleasant shock. She ran screaming from her husband's laboratory and never went near it again.

On December 28, Roentgen submitted a paper describing his findings, "On a new kind of ray," to a local scientific journal. Within days, news of the discovery was excitedly picked up by the press and spread like wildfire throughout the world, along with the instantly famous picture of Bertha's hand. People found the experiment easy to reproduce, and within months physicians everywhere were using the pictures it produced to set broken bones and to remove bullets and shrapnel. Over the single year following the discovery, more than a thousand technical and medical papers were published on the subject. With his new kind of rays, Roentgen had discovered a splendid window for looking within the living body and painlessly examining organs and bones.

For his work, Roentgen was offered a title, which he refused, and received numerous awards, including the first Nobel Prize in Physics in 1901. Soon after unveiling his discovery, Roentgen returned to his former research interests, and wrote only seven more papers. In October of 1914, he joined 92 other professors in issuing a manifesto in support of German militarism, an action that he later regretted. His family lost their wealth and suffered considerable hardship during the First World War and the depression that followed. After a short illness, during which he kept careful records of his own symptoms, Roentgen died in Munich on February 20, 1923.

Different imaging probes interact with different tissues in different ways and yield different kinds of medical information

Much of the information content of a medical image will invariably be irrelevant, or tend to detract from or obscure the diagnostically critical features – or worst of all, appear to be real but not be so. When confronted with the results of an X-ray, CT, NM, US, or MRI study, the viewer must detect any significant anomaly in it, regardless of how slight

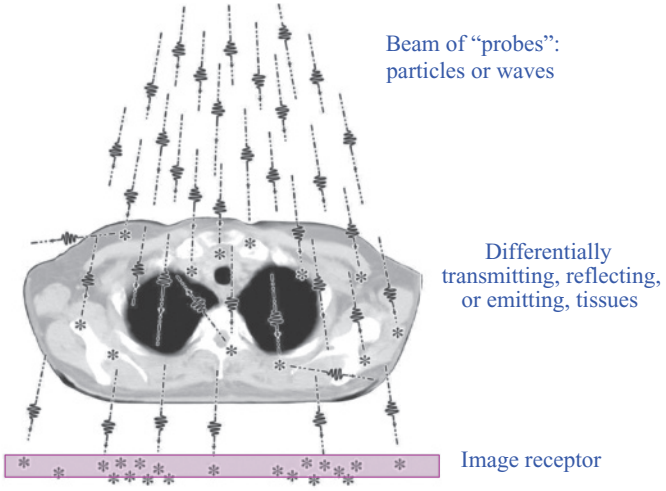

Figure 1.3 Creation of a transmission image of the body with a beam of X-ray probes, by keeping track of the fate of those that enter it and do, or do not, interact with it. An (ideally) uniform X-ray beam is directed at the chest; some of the X-rays incident on it are either absorbed or scattered through interactions with its atoms and molecules, predominantly in the dense bones. The differential attenuation of X-rays by the various body tissues is revealed in the (no longer uniform) residual beam emerging from its far side, and captured by the image receptor. This process is the basis for all X-ray imaging, including CT.

or well hidden it may be, and correctly identify a corresponding irregularity in the patient's body. She must then interpret this in terms of a deviation from normal anatomy or physiology — the what, how, and why of what has actually gone wrong with the cells, tissues, and organs. After determining the pathophysiology, she will hopefully be able to arrive at a reasonable differential diagnosis that ultimately enables selection of the best treatment.

A medical image will be considered good enough if it helps to achieve any or all of this — efficiently, reliably, safely, and, preferably, inexpensively. A diagnostic imaging system must therefore be able to display the specific, distinctive aspects of the patient's anatomy or physiology that are the cause of the problem, and be sensitive enough to pick up even very subtle early signs of the disease process. It may seem ironic that a "good enough" image is good enough, incidentally, especially since we so often strive for the "best." But there are likely to be hidden real costs from "better than good enough," especially *unnecessary* radiation dose, and the quality of the image itself is only part of the overall picture.

The specificities, sensitivities, and other characteristics of the various imaging tools, in turn, are determined by how they work — and they work in remarkably disparate ways. But while the imaging technologies make use of quite different physical processes in carrying out their appointed tasks, they do share a central, fundamental commonality of approach: they all gather information by creating, following, and recording, by some means or other, the transmission or reflections of suitable *probes* as they attempt to pass through a patient's body, or by monitoring the emission of signals coming from within it.

For transmission X-ray imaging, such as radiography, fluoroscopy, and CT, the body must be *partially*, but only partially, transparent to the probes (Figure 1.3). If the X-rays all slip through bones and organs without interacting with them, like light through a pane of clear glass, then no differences among the tissues can be visualized. Similarly, if their passage is completely blocked, nothing shows up. But if the probes are only somewhat affected – absorbed, scattered, reflected, delayed, whatever – we may be able to detect small differences in how they interact with the molecular constituents of diverse biological materials. And these small differences can then serve as the raw material for the creation of diagnostically useful images.

A beam of X-rays consists of such probes. X-rays are a form of electromagnetic (EM) radiation, as are gamma- and ultraviolet rays, visible light of all colors, infrared radiation, and radio waves. Physicists discovered a century ago that all of these display both wave-like and particle-like characteristics, if you know how to look for them; in the next chapter, we shall return briefly to this and other cases of what is sometimes called "quantum weirdness."

In the production of radiographs, however, only the particle-like attributes of EM radiation are relevant. You can think of an X-ray beam as

consisting of a stream of vast numbers of small, discrete, compact particle-like bundles of EM energy, called *photons*. X-ray photons travel in straight lines at the speed of light and, unless something absorbs or scatters them, they just keep on going. Most importantly when considering formation of an image, however, they can collide with atoms within the body, and in this way be removed from the beam.

When a fairly uniform beam of X-ray photons enters a chest, say, the skin, muscles, and bones attenuate it (i.e., thereby removing X-ray photons from it, and reducing its intensity) by different amounts, and in so doing cast a distinctive spatial pattern of X-ray shadows in it. The no-longer-uniform beam that emerges from the far side of the chest then falls upon and exposes an *image receptor*. In Roentgen's case, the first image receptor happened to be a sheet of cardboard covered with fluorescent material that glowed when his cathode ray tube was activated. Later he used a glass plate coated with a photographic emulsion that contained microscopic, transparent silver halide crystals; if sensitized by an X-ray photon, a crystal would transform into a minute speck of black pure silver when the plate was subsequently developed. The more X-ray photons that reached a part of the plate, the more silver halide crystals were altered, and the blacker, more visually opaque, that part of it became. Where absorption and scattering are relatively low, such as in the lung or the edge of the breast, more photons make it through to expose the image receptor, and the corresponding area on developed film appears darker. Conversely, the image of a bone, with its high beam attenuation, is much clearer, showing up brightly on a view box.

What is of interest in radiography (and fluoroscopy), and what is ultimately responsible for the patterns of clear and dark in a radiograph, is the three-dimensional (3D) distribution of the tissues within the body. What is recorded on film and available for diagnostic purposes is a 2D representation of the spatially varying X-ray intensity that was transmitted through the body. The radiographic process is thus a mapping, or condensation, if you prefer, of the patient's anatomy in three dimensions onto a two-dimensional visual map.

In *emission imaging*, the body itself may produce diagnostic signals naturally (thermography, electroencephalography, magnetocardiography), and image irregularities may indicate related health issues. Alternatively, a signal-emitting substance may be introduced into it intentionally (radiopharmaceuticals in PET, fluorescent dyes in infrared imaging); the tracer is designed to be taken up nonuniformly by the various tissues, and their spatial distribution is subsequently revealed by differential emission captured in the resultant images.

Ultrasound employs another approach, namely the *reflection* of the probes. A *transducer* generates high-frequency (1−10 MHz) mechanical vibrations and, when it is pressed against the skin, these initiate US waves that propagate through tissue. When the US energy comes to a boundary between tissues of different mechanical properties, however, it bounces back, like a tennis ball from a wall; the transducer senses these echoes upon their return to it, and transforms them into electrical signals that the computer untangles to create an echo-image.

MR imaging is something of an amalgam. It directs probes, radiofrequency (RF) electromagnetic waves, into the body which, under special conditions (including the application of a strong, constant magnetic field), will be absorbed by the hydrogen nuclei (protons) of tissue water and lipids. This interaction of EM waves with the protons leads to the emission immediately thereafter by the body of other RF radiation that is modulated by the behavior of these protons. The newer RF signal induces voltages in a wire pickup-coil, which are sent to the MRI's computer for image reconstruction.

In any case, regardless of whether these "probes" or "signals" are transmitted through, reflected in, or are emitted from the body or behave in some more subtle fashion, they go on to activate a probe-specific *image receptor* (IR) to create a medical picture. Older IRs, such as radiographic film and fluoroscopic image intensifiers, are said to be *analog* devices because they produce images that are continuous and smooth, like a photograph. A *digital* image, by contrast, can exist only in a computer system and monitor, and is comprised of a matrix of thousands or millions of tiny, distinct, square *pixels* of a discrete set of shades of gray or color. A digital system must be designed, incidentally, to ensure that these squares are small and numerous enough not to be individually noticeable, and that

Table 1.1 Typical values of the general characteristics of the principal imaging modalities: analog and digital radiography and fluoroscopy (R/F), and CT; nuclear medicine, including SPECT and PET; US; and MRI. These create images from probes such as X-rays transmitted through the body, gamma-rays emitted from within it, high-frequency sound waves reflected at tissue boundaries, and MRI radiofrequency waves that behave in more subtle ways. The different probes interact with tissues and image receptors by way of different physical mechanisms, and are influenced by different attributes of them. They are all effective at presenting some aspects of anatomy or tissue physiology or both, but they differ in the extent to which they can reveal either contrast among tissues or fine detail.

Modality	*Probe/signal*	*Detector*	*Source of contrast: Δ . . .*	*Anatomy/ physiology*
Analog R/F	X-rays through body	Screen + film; II + CCD	x, ρ, Z, (kVp)	A
Digital R/F; CT	X-rays through body	AMFPI; CsI array	x, ρ, Z, (kVp)	A
Nuclear medicine, SPECT; PET	Gamma-rays from body; 511 keV	NaI single crystal; BGO array	Radiopharmaceutical uptake	P
US	MHz sound	Piezoelectric transducer	ρ, κ	A
MRI	RF, magnet	AM radio receiver	Proton spin relaxation	A, P

Δ . . . , "differences in . . . "; x, tissue thickness; ρ, density; Z, atomic number; kVp, tube potential; II, image intensifier; CCD, charge coupled device; AMFPI, active matrix flat panel imager; κ, tissue elasticity; RF, radiofrequency EM.

the gray-scale levels are close enough together to appear smoothly graded.

Whether point-by-point on film or pixel-by-pixel for CT, the image receptor transforms the pattern of probes or signals that actually reach it into a visual image. The resultant image can be highly informative about healthy or diseased patient anatomy (radiography; CT), or about functional pathophysiology (nuclear medicine, including SPECT and PET; US), or both (MRI).

Some characteristics of the major imaging modalities are summarized in Table 1.1.

Twentieth-century (analog) radiography and fluoroscopy: contrast from differential attenuation of X-rays by tissues

When a patient shows up at her door today, a physician will perform a history and physical examination, and perhaps order and evaluate pertinent laboratory data. From her interpretation of the results, she can develop a tentative differential diagnosis. Medical imaging may now step in to play a decisive role in confirming or refuting a challenging differential diagnosis, and it may lead directly to a refinement of the final diagnosis. Imaging may also be invaluable in guiding treatment and in following disease progression or response.

X-ray film of a cracked phalange

The easiest of the modalities to describe, and still the most widely used around the world (away from modern medical centers) is conventional screen-film radiography.

Zea W. is a slender, elegant 18-year-old accomplished scholar and figure skater, and also the only daughter of one of the authors (A.B.W.). She's also tougher than she looks: several years ago, she was one of only two girls on her high school's JV ice hockey team. In a collision, however, a misplaced skate blade crushed the left hand, causing a great deal of pain, rapid swelling, and a brief and highly embarrassing burst of tears. After carefully inspecting the hand, the emergency room physician at the local clinic sent the patient to the radiology suite for an X-ray. If no bones were damaged, then Zea could get by with conservative management such as the elevation of her hand, intermittent application of a cold pack, and medications to reduce the swelling and discomfort. If the radiologist found a hairline fracture, the hand might need a cast to counteract any stresses on the injury during healing. If a bone had been broken into separate pieces, it might even necessitate wiring them together

surgically for proper setting. Before there were X-ray images, a physician would have to place a limb in a cast without being able to see clearly how to position the bones, and that could result in weakness and deformity after healing.

The clinic's digital X-ray system was under repair, so it was necessary to revert to an old film unit. The entire procedure took less than five minutes. The radiologic technologist (also known as a radiographer) protected Zea's entire body and neck with a lead-lined apron, which strongly absorbs any stray X-rays. He positioned her hand on a light-tight cassette, within which resided a sheet of specialized photographic film (Figure 1.4a). He then adjusted the height of the X-ray tube above it, and reduced the dimensions of the rectangular X-ray field (indicated by a coincident light field) until it barely covered the hand. He stepped behind a shielding wall, set the controls of the X-ray machine, and kept watch on his patient through a lead-glass window as he shot the film. He then replaced the exposed film with a fresh one, repositioned the hand, and made a second image.

The films were developed, ready for inspection. Both were of adequate quality for the radiologist to identify the problem, and so to guide the patient's treatment. As with nearly all radiographic studies, the contrast between bone and soft tissue was very good. High attenuation by a bone leads to a pale area on film, giving a "negative" appearance of the skeletal structures, with the surrounding, more radiolucent, soft tissues showing up darker. There was no visual noise in either film, and they had sufficient sharpness and resolution of detail to reveal a clean, simple break in one of the bones into two separate pieces, indicated by the arrows in Figure 1.4b and c. The radiolucent line corresponds to the fracture, with an interruption of the dense cortex that enabled X-rays to cross without as much absorption. These pieces had not been significantly displaced relative to one another, but the treatment required a cast to immobilize the bone, allowing it time to heal by consolidation with callous formation.

A month later, Zea was back on the ice.

Meanwhile, a lot was going on behind the scenes. In creating a radiograph, the real action occurs in three places – the anode of the *X-ray tube*, the *patient's body*, and the *image receptor*. In that order . . .

Generating the beam at the anode of the X-ray tube

A typical modern X-ray tube is a highly-evacuated container, made of glass or metal, within which reside two metal *electrodes*, a *cathode* and an *anode* (Figure 1.5a). The cathode consists of a thin tungsten metal filament housed within a focusing cup; a dedicated, low-voltage power supply drives current through the filament and heats it white-hot, so that it "boils" off electrons.

Almost all of the time, the *exposure* or *"beam-on" switch* is *open*, so that there is no electrical current from cathode to anode, in which case that's the end of the story. During the brief fraction of a second that the exposure switch is held *closed*, the cathode and anode become attached to the negative and positive poles, respectively, of a *generator* of very high, constant electric potential, which acts somewhat like a high-voltage battery (Figure 1.5b). For historical reasons, the potential applied across the tube is known also as the *peak kilo Voltage* (*kVp*), and most X-ray images are produced in the 60−120 kVp range.

The electrons boiling off the negatively charged cathode are accelerated to great velocity toward the positive anode. When they crash into it, something like $\frac{1}{2}$% of their collective energy is transformed into highly energetic X-ray photons; the rest becomes non-productive and potentially destructive heat that must somehow be removed rapidly from the anode and tube.

The result of all this is that a nearly uniform, rectangular beam of X-rays exits the tube via its *window* and heads off toward, say, a patient's hand.

The process brings to mind the time Fluffy curled up a little too close to your favorite Ming treasure (Figure 1.5c). As the vase accelerated downward, its gravitational potential energy transformed smoothly into kinetic energy of motion; when it crashed, most of its kinetic energy was expended abruptly in shattering it into tiny pieces, heating them, and scattering them in all directions – but a small amount was radiated away as sound energy. Same sort of thing happens here with the electrons at the anode.

Contrast from differential attenuation of the beam within the body

Contrast is the principal measure of the extent to which tissues that are anatomically or

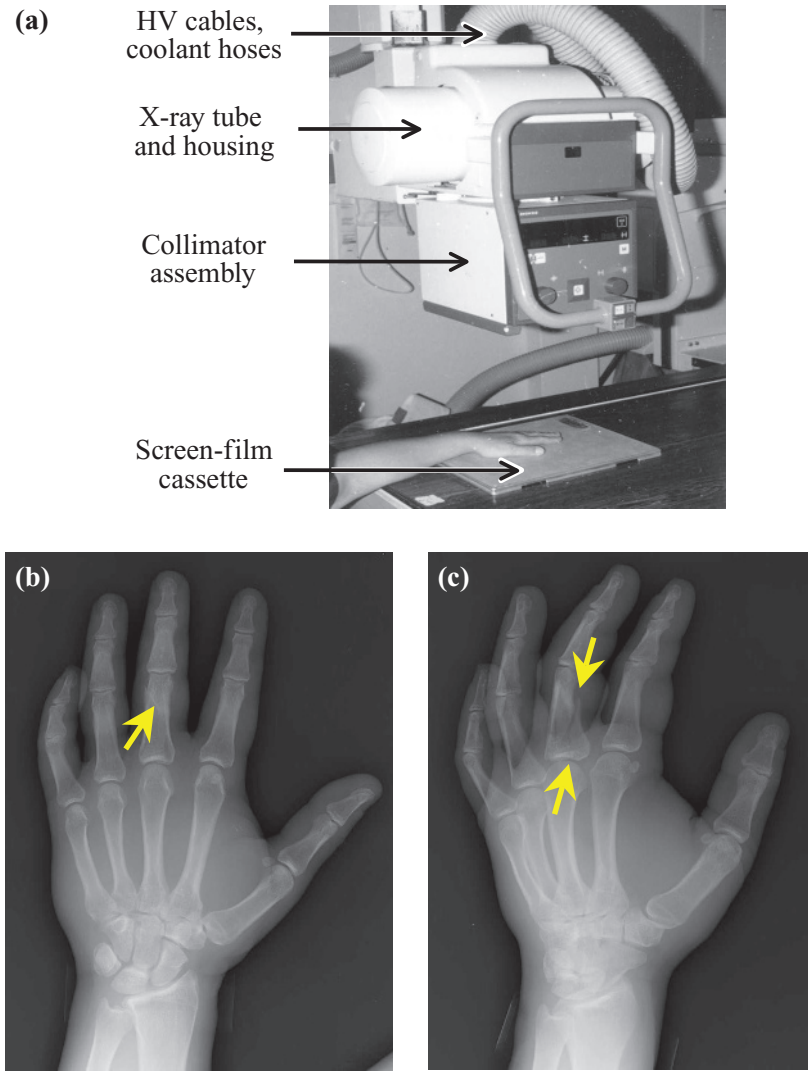

Figure 1.4 X-ray study of a hand. (**a**) A screen-film X-ray unit, with the X-ray tube (inside the horizontal, white cylindrical housing) pointing its beam downward at the hand, which is resting on a film-cassette image receptor. Apart from the X-ray window, the tube is surrounded with lead for radiation protection. The corrugated white tubing carries the *high-voltage cables* from the *generator*, which is outside the room, and hoses for circulating *coolant oil* around the tube. The two knobs on the front of the *collimator assembly* allow adjustment of the beam size, to minimize the volume of tissue that has to be directly irradiated; this also cuts down on the amount of *scatter radiation* produced, which would otherwise both degrade image quality and contribute additional non-productive dose to the hand. Only some of the X-ray photons pass through to darken the film and create a shadowgram; the rest are scattered or absorbed, predominantly in the bones. (**b**) The developed film displayed sufficient image *contrast* and *resolution*, and low enough visual *noise*, to reveal clearly a slightly displaced, oblique fracture of the proximal phalanx of the third finger of the left hand (arrow). (**c**) The same fracture line is better demonstrated in the oblique projection, showing how it extends proximally to the proximal metaphysis of the proximal phalanx to the level of the articular cartilage of the metacarpo-phalyngeal joint (arrows). This has therapeutic implications and demonstrates how one must obtain several views (preferably orthogonal) of the target region, since a 3D structure will project on the film only in 2D.

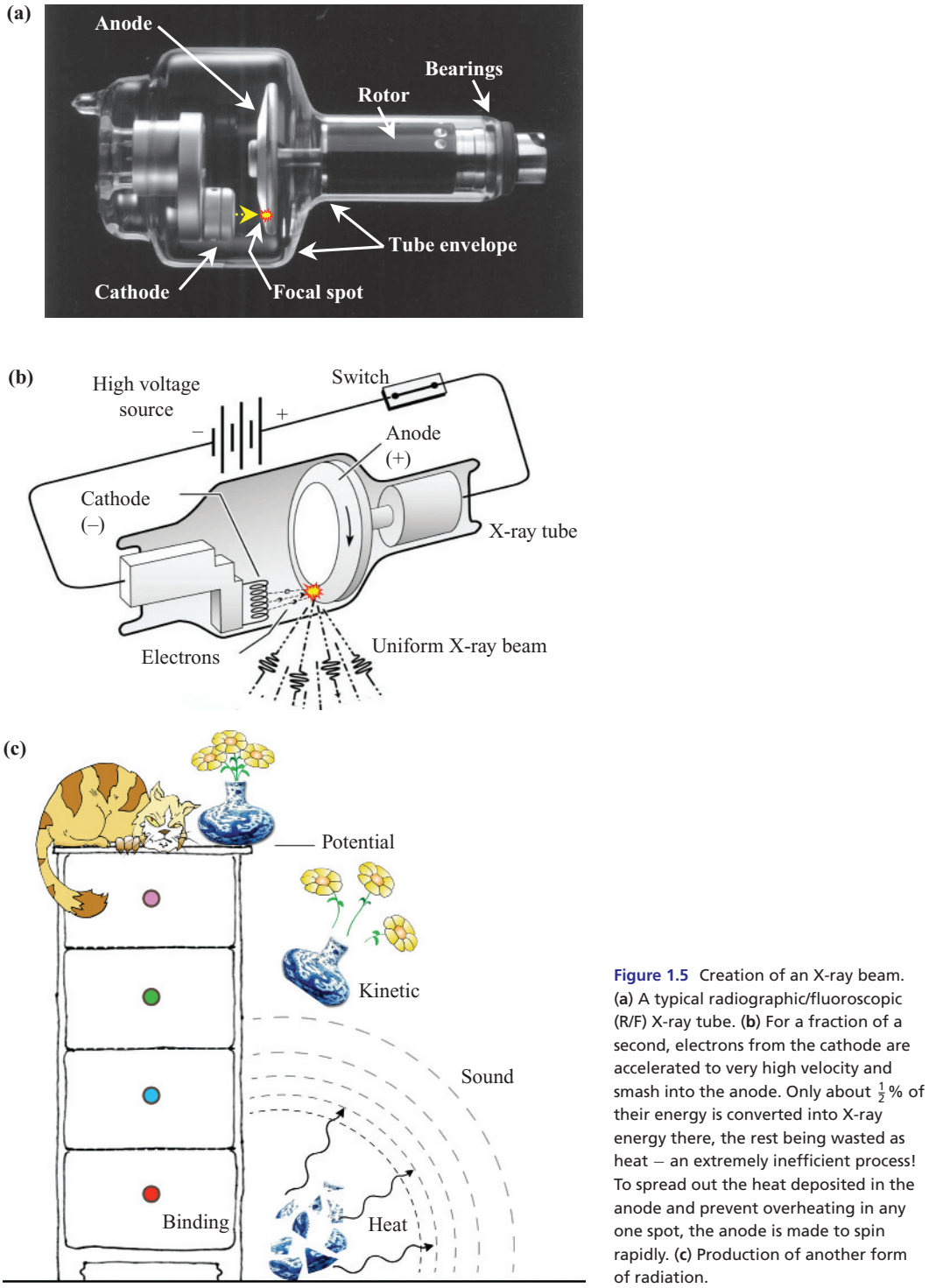

Figure 1.5 Creation of an X-ray beam. (**a**) A typical radiographic/fluoroscopic (R/F) X-ray tube. (**b**) For a fraction of a second, electrons from the cathode are accelerated to very high velocity and smash into the anode. Only about $\frac{1}{2}$% of their energy is converted into X-ray energy there, the rest being wasted as heat – an extremely inefficient process! To spread out the heat deposited in the anode and prevent overheating in any one spot, the anode is made to spin rapidly. (**c**) Production of another form of radiation.

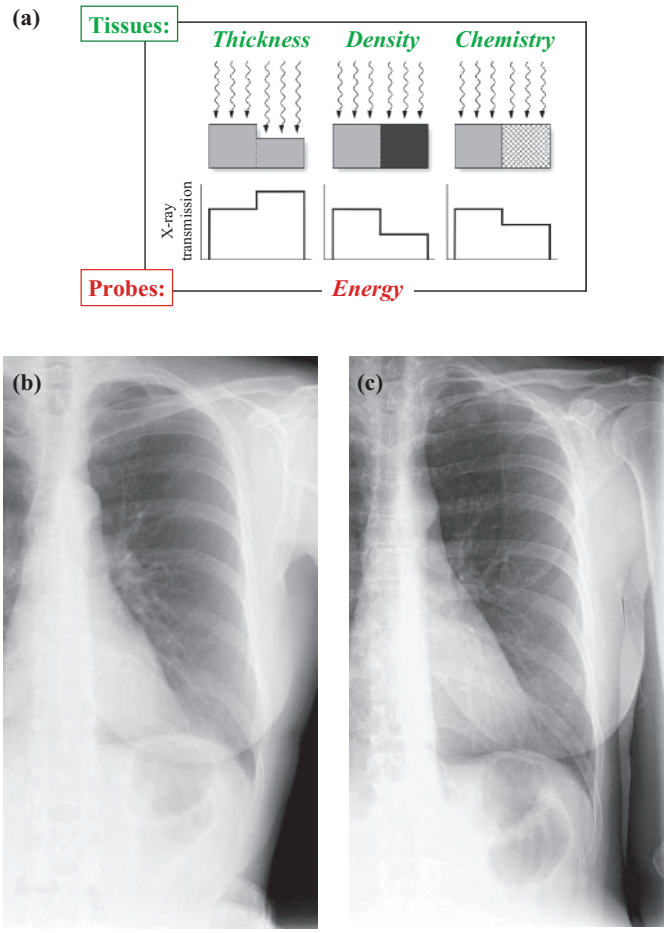

Figure 1.6 X-ray contrast. **(a)** For X-rays, three primary determinants of contrast are *differences* in the thicknesses of tissues, in their densities, such as between lung, muscle, and bone, and in their chemical makeup. **(b)** A fourth important influence on subject contrast is the effective energy of the X-ray beam, as determined by the setting the adjustable *kVp*. This PA image of the left lung of a patient presenting with chest pain was taken at 110 kVp. **(c)** When more detail of the ribs is needed (as in the search of fractures following trauma), then a lower applied voltage, such as 70 kVp, is selected. (b) and (c) modified from the Teaching File images of the American College of Radiology (ACR).

physiologically different appear as such in an image. While other aspects, like resolution or noise level, can be especially important in certain studies, usually it is the visual contrast in a diagnostic image that allows the viewer to distinguish among and examine organs and other tissues, both normal and pathological.

With X-rays, various types of soft tissue and bone absorb and scatter a beam's photons at different rates, which is responsible for the contrast. The amount of attenuation of the beam along any geometric "ray-path" through the body, in turn, depends on the thicknesses and densities of the materials it traverses, and on their chemical compositions (Figure 1.6a). The consequent *differential attenuation* of the beam imprints an X-ray shadow in it, and it is the two-dimensional pattern of X-ray intensity emerging from the far side of the patient, the *primary X-ray image*, that is subsequently captured by the image receptor (IR).

The amount of X-ray contrast among tissues in an image is thus governed primarily by the *differences* in attenuation along the countless ray-paths, hence by the relative *differences* in tissue thicknesses, densities, and chemical makeup of the tissues.

Rates of attenuation, hence amounts of contrast, can be affected strongly also by the setting of the kVp applied to the tube. It may be possible to improve subject contrast for a specific clinical task by selecting a more appropriate kVp (Figures 1.6b and c), but probably at the price of greater radiation dose to the patient.

Radiography can provide excellent contrast for locating and viewing objects that have densities

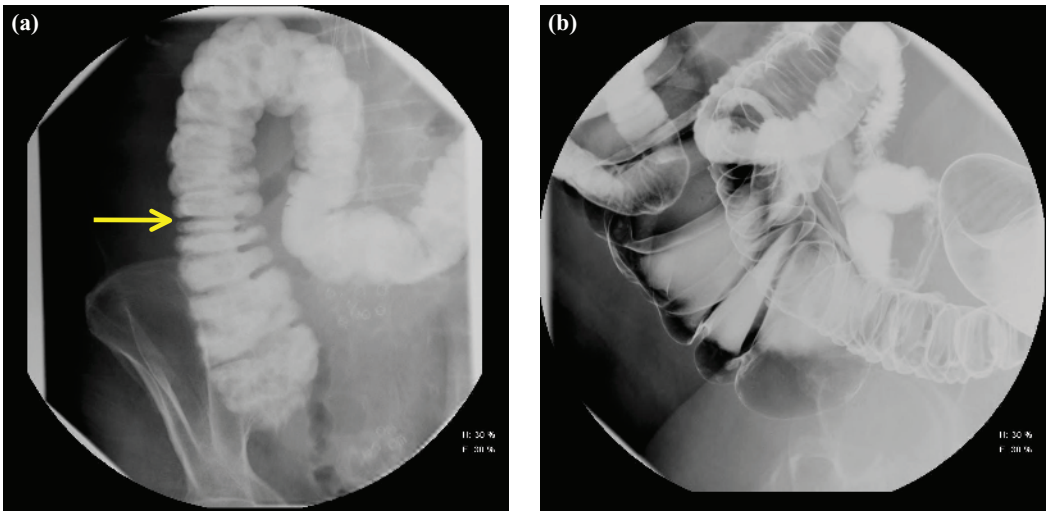

Figure 1.7 Fluoroscopic examination of the GI tract with contrast agent. **(a)** In a barium enema study, a suspension of barium, which is unusually effective at absorbing X-rays, will opacify the lumen of the colon after being administered per rectum, enabling the examination of its diameter and contours. In this image centered at the level of the cecum, one can see areas of normal narrowing of the colon called *haustrae* (arrow), along with abnormal projections from the lumen such as diverticula or filling defects such as polyps. **(b)** A radiolucent material such as insufflated air can then be introduced to fill the lumen of the colon. The remaining barium coats the colonic wall, which is now distended, giving a *double contrast* study, enabling viewing of the partially translucent bowel *en face*.

or chemical makeup significantly different from those of the surrounding tissues — as with bullets, bones, or fluid or masses in lungs. Subject contrast among similar soft tissues, however, can sometimes be barely discernible. Because its density and other properties may be close to those of nearby healthy tissues, a cancerous growth also may give rise to little radiographic contrast. Still, a lesion may reveal its presence through a *mass effect*, displacing or otherwise altering the appearance of an adjacent structure (such as the wall of a bowel coated with barium contrast agent) that *can* be visualized.

The contrast for some tissues can be enhanced artificially by altering their physical properties with a *contrast agent*. Because iodine atoms happen to absorb X-rays especially strongly, blood vessels containing intravenously injected iodine compounds tend to stand out clearly from the surrounding soft tissues. Barium has similar application for fluoroscopy of the esophagus, stomach, and intestine (Figure 1.7a). Following a barium enema, moreover, air can be infused into the colon and function as a second kind of contrast agent because air does *not* soak up X-rays (Figure 1.7b).

Alternatively, it may well be appropriate to turn to another modality. Even when almost nothing shows up on film or DR, for example, CT may adequately depict the organs of interest. Likewise, US may quickly and inexpensively distinguish between a cyst and a solid lesion and, in addition, it poses no radiation risk. And in many situations MRI can create soft-tissue contrast far better than that of CT, also with no dose of ionizing radiation. But however you do it, the critical objective is normally to generate enough relevant image contrast to allow a good clinical diagnosis.

The usefulness of an image may depend not only on the degree of contrast it displays among tissues, but also on its *resolution* or *sharpness*, and on the level of interfering *visual noise* or *artifacts* that might be present. Some of these will be of greater importance than others in a given medical situation. The search for tumors requires the high contrast offered by SPECT and PET, for example, but these deliver poor resolution – which, however, is not a problem for this application. The inherently high resolution of X-ray films and digital radiography, on the other hand, enables them to provide critical details

of fine structure, revealing hairline cracks in bone, microcalcifications in breast, and irregularities in narrow blood vessels made visible with iodine contrast agent. And while visual random noise plays almost no role in radiography, it can be a dominant factor in CT, nuclear medicine, US, and MRI.

Exposure of a screen-film image receptor

The third step in creating a radiograph is to transform the *subject contrast* in the primary X-ray image emerging from the patient into visible *image contrast* in a permanent record in the IR.

Not many X-ray photons manage to pass completely through the body, as it happens, but a good fraction of those that do are captured by the image receptor. In traditional analog radiography, the IR is a sheet of photographic film sandwiched between the two flat *fluorescent screens* of a light-tight *radiographic cassette* (Figure 1.8a). When an X-ray photon strikes an atom in a transparent microcrystal of fluorescent material in a screen, its energy is converted into a pinpoint flash of thousands of visible light photons (Figure 1.8b).

Many of the light photons created this way head into the adjacent sheet of film. The two surfaces of standard film are coated with thin layers of *emulsion*, which contains a suspension of translucent microcrystals composed of a mix of *silver bromide* and *iodide* plus trace amounts of other goodies (Figure 1.9a). If a half dozen or more light photons from a screen happen to strike a particular silver halide microcrystal, then it will become *sensitized* and, during the subsequent chemical *development* of the film, it will be transformed into a minute black fleck of nearly pure silver (Figure 1.9b). Crystals in the emulsion that are *not* sensitized in this fashion will be dissolved and removed from the film during fixation and washing.

In this fashion, a single X-ray photon striking a fluorescent screen typically results in a microscopic black cluster of hundreds of minute specks of silver. Where more radiation passes through the patient and reaches the cassette, there arises a higher spatial density of these opaque dots. Here, the developed film is darker, with a higher *optical density* (OD). The pattern of X-ray photons emerging from the patient is thus distilled into a permanent visible record, to be placed on a view box for inspection.

The reason for the fluorescent screen is that the indirect two-step process, X-ray-to-light and then light-to-film, is greatly more efficient than direct X-ray-to-film. With screens, the IR requires one or two orders of magnitude less radiation to achieve a usable average OD, with a correspondingly lower *dose* to the patient. There is, however, a significant trade-off: thicker and therefore more sensitive screens may reduce patient dose, but they also lower resolving capability, and the solution to this dilemma must rely on clinical considerations.

To summarize: transmission X-ray imaging involves the *differential attenuation* of a previously flat X-ray beam through interaction with the various tissues, followed by *differential exposure* of the image receptor. This is true for all X-ray imaging, whether screen-film or digital planar, or CT, or fluoroscopy.

Image intensifier-based fluoroscopy with a CCD/CMOS electronic optical camera

Fluoroscopy is radiography's first cousin, the clever one that lets the physician watch continuously changing processes live in real time as they take place, rather than as one or a few radiographic snapshots developed later. To achieve this, it employs a more complex image receptor (Figure 1.10).

The X-rays that pass through and emerge from the patient do not expose a film cassette but rather, in most fluoro systems, they project directly onto the front face of an *image intensifier* (II) tube. An II is an electronic vacuum tube device that can transform a life-sized, very faint pattern of X-ray energy into a small, bright corresponding pattern of visible light. The output of the II tube used to be photographed directly with a still or cine film camera or viewed with a TV camera. These days, a solid state electronic *charge-coupled device* (*CCD*) or a *complementary metal oxide semiconductor* (*CMOS*) optical camera does the job.

As with X-ray filming, fluoroscopy is most adept at distinguishing objects that differ significantly from soft tissue in either density or chemical constitution — such as the passage of intravenously injected iodine-based contrast agent to or through constrictions in blood vessels, or the movement of barium past partial obstructions in the GI tract.

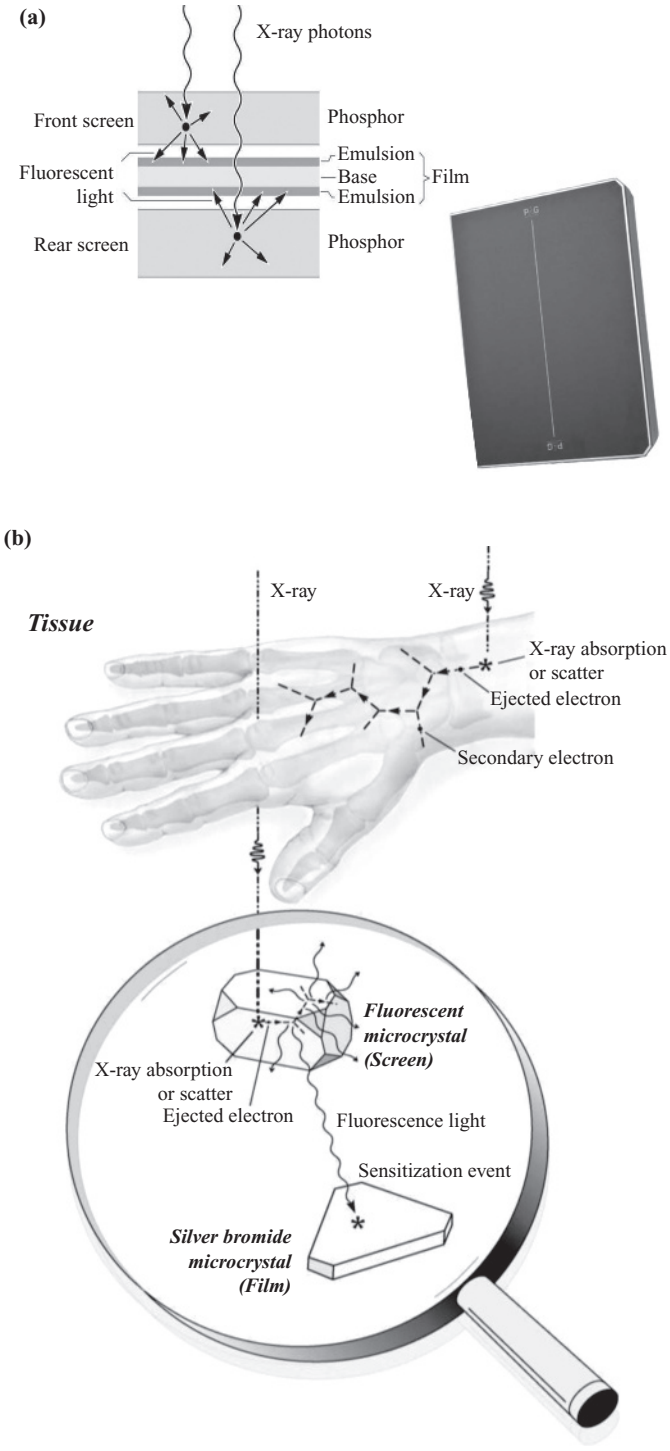

Figure 1.8 A screen-film X-ray image receptor. **(a)** The cassette consists normally of a pair of fluorescent screens in a light-tight, mechanically rigid housing; it can be opened in a darkroom to insert or remove film from between the screens. This cassette contains an embedded anti-scatter grid for easier and quicker imaging. Photograph courtesy of Reina Imaging. **(b)** An X-ray photon that happens to pass through the body and then strike a fluorescent microcrystal in the screen will excite it; the crystal relaxes immediately thereafter with the emission of thousands of visible light photons that will expose the film.

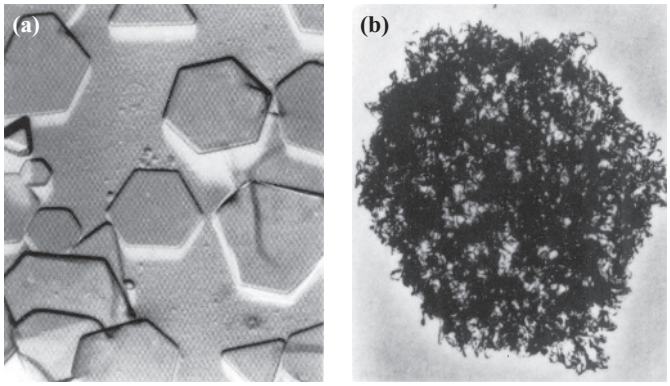

Figure 1.9 What makes photographic film dark? (**a**) A dispersion in the emulsion of tiny translucent microcrystals of silver iodobromide, seen here with the aid of an electron microscope. Several light photons striking a silver halide microcrystal will activate, or sensitize, it such that (**b**) upon chemical development, it transforms into a microscopic, opaque speck of silver metal, one of which is shown here. Courtesy of Arthur Haus, Eastman Kodak Company.

Fluoroscopy can also guide the removal of a radiopaque body from within the body, such as a bullet or urolith, or the insertion of one into it (e.g., a catheter or stent).

With most systems, the X-ray tube points upward from beneath the patient table (Figure 1.10a). It may be possible to tilt the whole assembly upward, including the table, for imaging the patient in the vertical orientation. Alternatively, as is standard in modern angiography suites, the X-ray tube and image receptor are held at opposite ends of a rigid *C-arm* support, as in Figure 1.10b, that can be rotated about one or more axes.

Modern angiography units are replacing the bulky, unwieldy II tube plus camera combination with a much thinner, lighter, and more maneuverable solid-state *active matrix flat-panel image* (AMFPI) receptor. A flat panel IR, the technology of which evolved from that of liquid crystal and plasma display monitors, makes things digital from the outset but currently at considerably greater cost. The most advanced interventional/angiographic

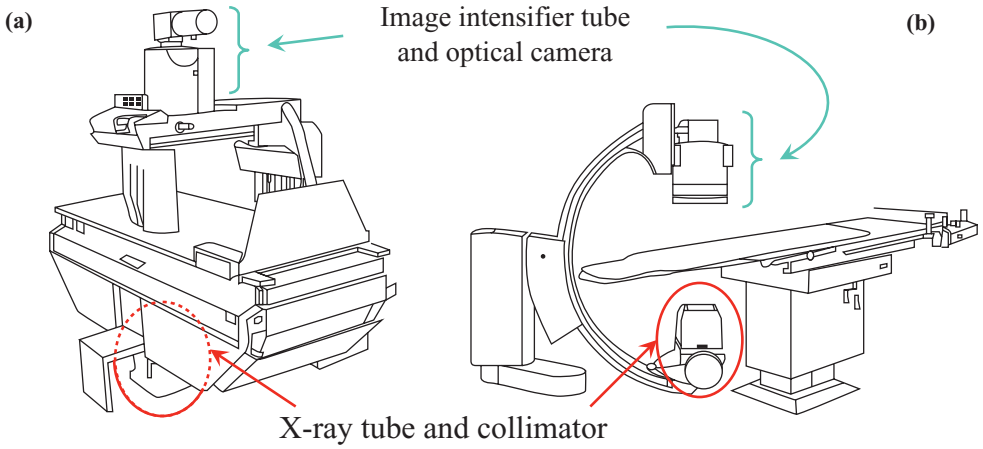

Figure 1.10 With fluoroscopy, the X-ray image receptor is an image intensifier (II) plus electronic optical camera combination, rather than screens and film. The X-ray beam is pulsed rapidly, but each pulse is of much lower intensity than for radiography. (**a**) With a standard radiography/fluoroscopy (R/F) system, the X-ray tube lies below the patient table, so that the lead-lined curtains surrounding it will cut down on scatter dose to the operators near the machine. The image receptor views the patient from above. The signal from the camera may be digitized and fed into a computer, making possible quasi-digital fluoroscopy and digital subtraction angiography. (**b**) An angiography device is mechanically more flexible and complex. The X-ray tube and image receptor (where, in the more advanced and totally digital systems, a solid-state *active matrix flat-panel imager* replaces the II tube and CCD pair) reside on opposite ends of a *C-arm* support that can be rotated about up to three axes. Modified from Bushberg JT, Seibert JA, Leidholdt, Jr. EM, Boone JM, *The Essential Physics of Medical Imaging*, 2nd edn, Philadelphia, Lippincott, Williams, and Wilkins (2002), fig. 9-15.

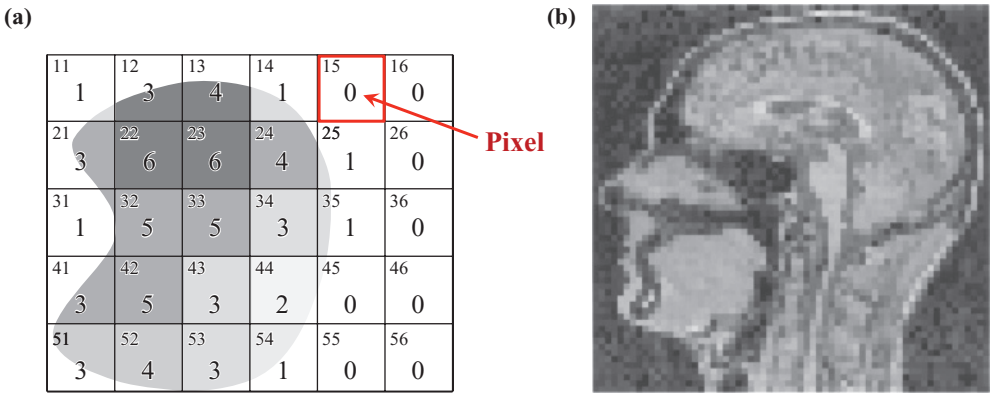

Figure 1.11 Two-dimensional digital image. (**a**) The number in the upper left corner of each pixel, or picture element, is its *pixel address*. The larger, central number represents the *pixel value* – that is, the degree of brightness, averaged over the entire pixel, where (in this example) the number 0 refers to the lightest and 6 is the darkest. The image can then be presented as a single string (i.e., a *one*-dimensional representation) of pixel addresses coupled with the corresponding pixel values. (**b**) The importance of many, small pixels and enough shades of gray. This MRI image of a head utilizes 256 shades of gray, which is OK, but only a 64 × 64 pixel matrix, which does not provide sufficient resolution. Courtesy of WS Kiger, III, Massachusetts Institute of Technology.

biplanar systems support two X-ray tubes and two flat panels, a configuration that allows simultaneous antero-posterior and lateral observation of the patient (or with other pairs of angles); such orthogonal imaging is often helpful in making visual sense of three-dimensional, tortuously complex vascular, biliary, and renal structures.

Twenty-first century (digital) images and digital planar imaging: computer-based images and solid-state image receptors

Conventional X-ray radiography is still the most common, and least expensive, way of obtaining diagnostic medical and dental images, and often it is perfectly adequate. But modern imaging departments have other options from which to choose – and just about all are built around computers.

Computers are invaluable for image enhancement with II-based fluoro, planar NM, and US. They are absolutely essential, moreover, for image generation with CT, MRI, CR, DR, SPECT, and PET. But either way, for computers to work their wonders, an image must be present in digital form.

Digital images

Creating a digital image is like the converse of painting by numbers. In simplest two-dimensional form, the computer partitions an image, obtained somehow with an image acquisition device, into an imaginary 2D array or *matrix* of many small square *pixels* (*pic*ture *el*ements), each corresponding to a tissue *voxel* (*vo*lume *el*ement) within the patient's body. Every pixel is assigned a unique *pixel address*, or numerical spatial location; the associated *pixel value* is the number that corresponds to the value of the biophysical parameter being assessed in the voxel. The matrix addresses for the 30-pixel matrix of Figure 1.11a, for example, consist of pairs of integer indices, where the first and second label the five rows and six columns of the matrix, respectively, such as 11, 12, 13, 14, 15, 16, 21, 22, . . . , 55, 56. The range of degrees of brightness on a black-and-white monitor is referred to as the *gray scale*; each pixel's gray scale level is set to correspond to a specific pixel value, in this case with a range from 0 to 6; the same general approach would apply to a color display. The entire image can then be represented as a long *one*-dimensional string of the addresses and corresponding pixel value numbers, such as: 11-1; 12-3; 13-4; 14-1; 15-0; 16-0; 21-3; 22-6, . . . , 55-0, 56-0. Perhaps a very simple form of *image compression* comes to mind that greatly reduces the amount of data that must be retained in such a string.

There are two digital imaging technologies that have been rapidly displacing screen-film radiography. Computed radiography (CR) is relatively

simple and inexpensive, and employs an IR that is similar to a screen-film combination, but one in which the active element is developed electronically, rather than chemically. Digital radiography (DR) is more advanced and much faster. A DR image receptor is built around an active matrix flat panel imager, which consists of several million independent sensors, each capable of determining the local X-ray intensity. With the sensors arranged as a 1024 × 2048 matrix, for example, there would be about two million pixels, and two million numbers would be required to represent the shades of gray of those two million pixels in a complete digital encoding of an image.

There are great advantages of both DR and CR over film, such as the capacity for image processing, rapid storage, and instantaneous communications, and Chapters 6 and 7 will cover these extensively. The same is true for digital fluoroscopy and digital subtraction angiography, which can capture events changing in real time far better than systems based on II tubes.

For MRI, the pixel matrix is most likely to be 512 × 512, requiring less computer memory to store an image, but considerably more calculational power to generate it in the first place. Troubles can arise, as with any other digital modality, if the pixel size is not handled properly: Figure 1.11b was reconstructed, for example, with a 64 × 64 grid, instead, an example that exaggerates the difficulty, but the pixelation would likely still be noticeable even at 256 × 256. Other problems arise if there are not enough distinct shades of gray, or if all the pixels are all shown somewhat too dark or too light – that is, if improperly *windowed*.

Computed tomography: three-dimensional mapping of X-ray attenuation by tissues

Conventional radiographic and fluoroscopic images are relatively easy to produce. But the superimposed shadows from overlapping tissues may obscure the critical details that the physician needs to see — the shadows from an intricate three-dimensional structure can project into hopeless two-dimensional disarray on film or with CR and DR.

The idea behind CT is straightforward, and was described in connection with Figure 0.1. CT creates, digitizes, and stores in a computer the radiologic images from a large number of different perspectives.

Imagine a patient as comprised of many thin transverse slices. In the early days, CT generated an image of the tissues within only a single slice 1 cm or so thick, for technical reasons, but now it is most common to scan the patient with 64 slices each 0.5 mm or so thick, all at the same time (Figure 1.12a).

It is perhaps easiest to visualize the operation of a CT by considering the first commercial head scanner, produced by the British company EMI (Figure 1.12b). It swept a very narrow "pencil" beam of X-rays across the head, in a direction perpendicular to the beam orientation, while monitoring the amount of energy transmitted through it, at 160 points along the way, with a small, co-linear X-ray detector, also being shifted sideways (Figure 1.12c). It then rotated the tube plus detector assembly rigidly 1° around the patient, and repeated. This set of motions is known as "translate/rotate" data acquisition, and the first and 60th such scans are shown. After the accumulation of data from 180 angles, the computer then worked backward through vast numbers of complex calculations to *reconstruct* and display the spatial distribution of the materials (or, more precisely, of the X-ray attenuation properties of the materials) that must have been responsible for this particular set of images. Obtaining the data and reconstructing a single slice of the head took over four minutes.

The patient table was then advanced 1 cm or so, and the entire procedure carried out again to produce the next, adjacent slice. The resulting information was shown as a sequence of images of individual thin transverse slices of tissue (Figure 1.12d). This slice happens to display a *star artifact* caused by the inability of the CT's computational *reconstruction algorithm* to deal with the abrupt change in rate of attenuation that occurs at a small metal aneurysm clip.

By eliminating the interfering patterns that come from over- and underlying bones and organs, CT provides ample contrast among the various soft tissues, far better than standard radiography or fluoroscopy can do. So CT is routinely used for detailed studies of abdominal and pelvic organs, the lungs,

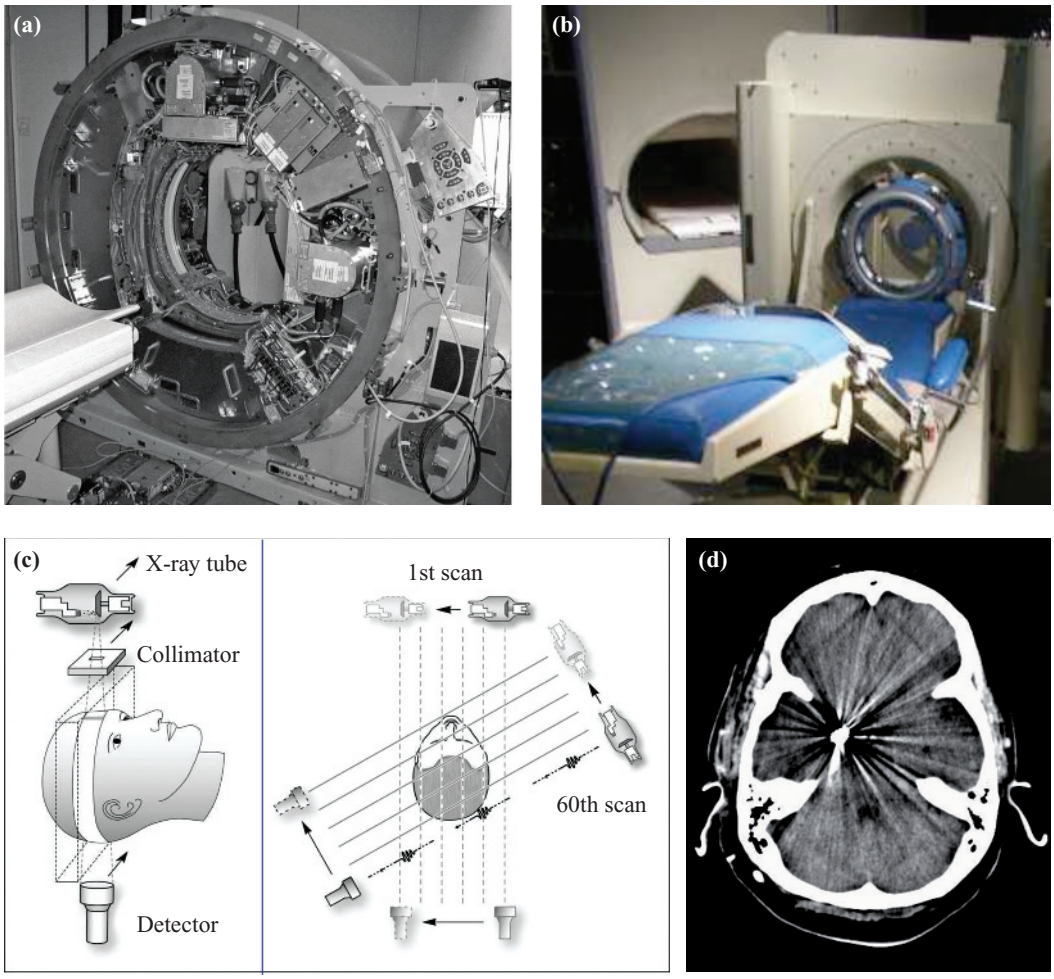

Figure 1.12 CT data acquisition. (**a**) An immodest view of a modern dual-source, multi-slice CT scanner, with a pair of X-ray tubes at right angles and a corresponding pair of multi-slice detector assemblies. (**b**) The first commercial scanner, manufactured by the British company EMI, Ltd, with development funds provided largely by the Fab Four, also an EMI product. (**c**) The geometry of data acquisition by a first-generation CT device, such as the EMI machine, known as "translate-rotate." The tube and its narrow pencil beam of X-rays swept across the head, and a detector shifted so as to remain co-linearly with it monitored the intensity emerging from its far side. The tube plus detector assembly was then rotated 1° around the patient, and the procedure repeated; here are shown the first and sixtieth scans. (**d**) A transverse CT slice, with one of a number of types of CT artifacts, a "star" caused by a metal aneurism clip; there, the rate of X-ray attenuation changes abruptly from that of soft tissue, causing problems for the numerical calculations of the reconstruction algorithm. Reproduced from Flohr T, Schmidt B, Advances in CT. In: Wolbarst AB, Capasso P, Godfrey DJ, *et al.* (eds), *Advances in Medical Physics*, vol. 4. Madison WI: Medical Physics Publishing, 2012, fig. 4-5 (part a).

the brain, and just about everything else. CT can pick up physically dense objects of the order of 0.1 mm in dimensions, and its general resolution can be better than 0.3 mm. While this is not as good as the resolution in screen-film, CR, and DR, the greatly enhanced contrast may far more than make up for that.

A series of adjacent, thin transverse (axial) slice images can be stacked and melded together, to provide a truly three-dimensional picture (Figure 1.13a). On every slice, a *segmentation* program might automatically locate each interface between bone and soft tissue, say, where the rate of X-ray attenuation changes rapidly, and draw a contour

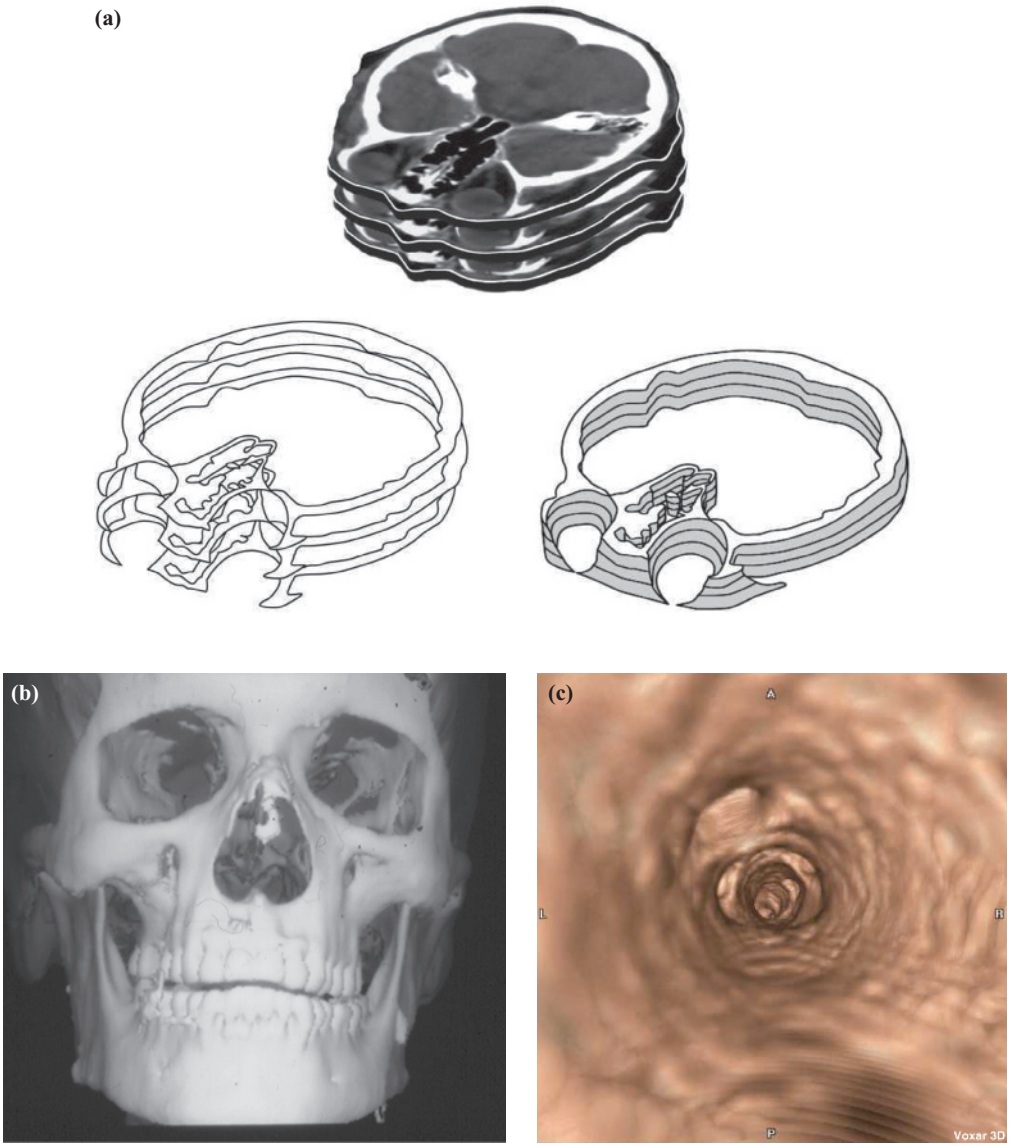

Figure 1.13 Three-dimensional display. **(a)** With CT and MR data acquisitions, slice-images can be stacked upon one another, enabling a reconstruction in three dimensions that can be manipulated (e.g., rotated) so as to offer the best view of a lesion. **(b)** Three-dimensional rendering of the skull (enclosed in 2200-year-old wrappings) of a former resident of Luxor, Egypt, who apparently died of natural causes. He is now part of the permanent mummy collection of the Smithsonian Institution, Washington, DC. Courtesy of Wayne Olan, George Washington University Medical Center. **(c)** Virtual abdominal aorta.

line there. It then assembles the curves in three dimensions, and tiles them optically so as to create a smooth cover representing bone surface. Finally, it can assign degrees of transparency and colors that depend on tissue type, and cast a beam of simulated light through the resulting volumes to give the impression of overlap and depth (Figure 1.13b). It's rather like creating a *papier-mâché* object by plastering paper over a chicken-wire framework, but here it's all done by the computer. Much of the technology that makes all this happen was developed by the animation industry, the military, and others.

The viewer can rotate, dissect, and otherwise manipulate lifelike, three-dimensional images, or display high-resolution coronal or sagittal thin slices. Virtual reality display technologies allow one to observe while traveling down the length of the esophagus, bronchus, intestinal canal, or aorta from within, without actually having to go anywhere near them (Figure 1.13c). It is even possible to watch the heart beating in slow motion, obtaining the images synchronized with the cardiac cycle (cardiac gating) and then replaying the images in a cine loop at the desired speed.

The full power of the approach can be appreciated in an attempt to read the fine details of a cranial fracture. In many cases, there is simply too much visual confusion from overlapping tissue structures to allow the detection and interpretation of slight irregularities with radiography (Figures 1.14). CT can often eliminate the chaos by, in effect, removing all of the body except for a single thin pancake slice of tissues.

MRI can do nearly all of this, too, sometimes providing far better soft-tissue contrast. Still, when either modality can perform a job just as well, then sometimes the considerably lower costs of CT, or the speed of helical, multiple-slice CT, or even just the more rapid access to a CT machine may make it the modality of choice. The major downside of CT is the relatively high radiation doses it involves, which have become a major health concern, especially for infants, children, and women during pregnancy.

Helical, multi-slice CT

In the mid-1970s, the arrival of CT made possible an entirely new way of seeing, and the resulting impact on patient care has been incalculable. Over the past two decades, CT has had to face stiff competition from MRI, which provides clinical information on soft tissues that is usually comparable, and sometimes far superior. This partly explains the development of *helical* CT machines capable of acquiring data much more rapidly by continuously translating the patient table through the gantry opening without having to stop and shoot each slice separately. Soon thereafter, *multi-slice* devices were designed with multiple independent rings, or belts, of tiny X-ray detectors, typically 64 but up to hundreds in some models, which make it possible to create numerous slices simultaneously. Modern helical, multi-slice machines can produce multiple adjacent thin (0.5 mm) slices of a region tens of centimeters long in a matter of seconds, and are now a mainstay of a modern imaging department.

Nuclear medicine, including SPECT and PET: contrast from the differential uptake of a radiopharmaceutical by tissues

Gamma-rays are inherently the same electromagnetic stuff as X-rays and, in medical applications, their ranges of energy overlap. The two, however, differ radically in their origins: gamma-rays are emitted from the unstable nuclei of certain radioactive atoms, while X-rays are created electronically inside an X-ray tube. It is the source of the radiation, not the radiation itself, that distinguishes the two.

Radiopharmaceutical = radionucleus + organ-specific agent

Nuclear medicine provides information that is primarily physiologic or functional in nature, rather than anatomic.

A standard nuclear medicine study makes use of a *radiopharmaceutical*, a chemical substance that consists of two components and displays both of two essential characteristics: one part of the substance is an *agent* that tends to seek out and concentrate preferentially within a particular biological compartment in the body, an organ or tissue of interest. The agent macroaggregated albumin (MAA) protein, for example, consists of microscopic particles (10–90 μm across) that lodge briefly within the patent microvasculature of the pulmonary arterial blood supply, making them suitable for imaging the vasculature (as opposed to the air volumes) of the tissues of the lung.

The other piece of a radiopharmaceutical is the radioactive atom, attached firmly to the agent, that undergoes spontaneous *radioactive decay*, with the creation of, normally, a single, high-energy gamma-ray photon (Figure 1.15a). The characteristics of the particular radionuclide *metastable technetium*-99 (Tc-99m) make it just about ideal for imaging, and it has long served as the standard workhorse isotope in nuclear medicine. Tc-99m has an energy sufficiently high to escape the body, but low enough

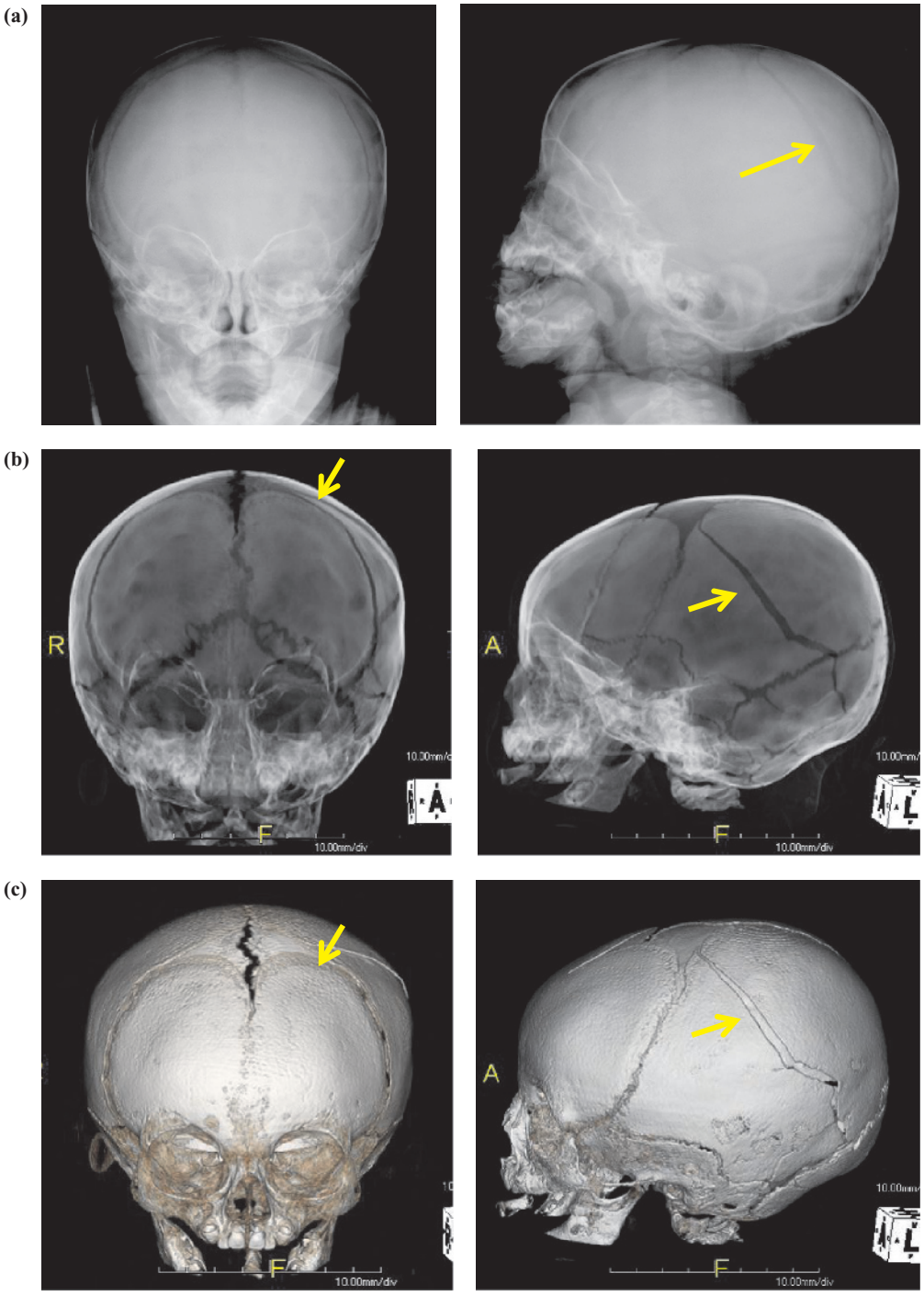

Figure 1.14 Three-dimensional CT or MRI imaging can make visible complex structures that would be obscured by overlying tissues on plain radiography. This case series involves an infant who suffered blunt trauma to the head. (**a**) Initial analysis in the emergency department was performed with AP and lateral radiographs of the skull. Questionable cortical defects on the left side appear on the AP image; these represent a linear fracture of the parietal bone, and are seen more clearly as a radiolucency on the lateral image (arrow). Next, the skull is captured with CT and displayed in both (**b**) a translucent and (**c**) a surface rendering. The CT images show more clearly the same non-displaced fracture extending from the anterior fontanelle across the lamboidal suture (arrows).

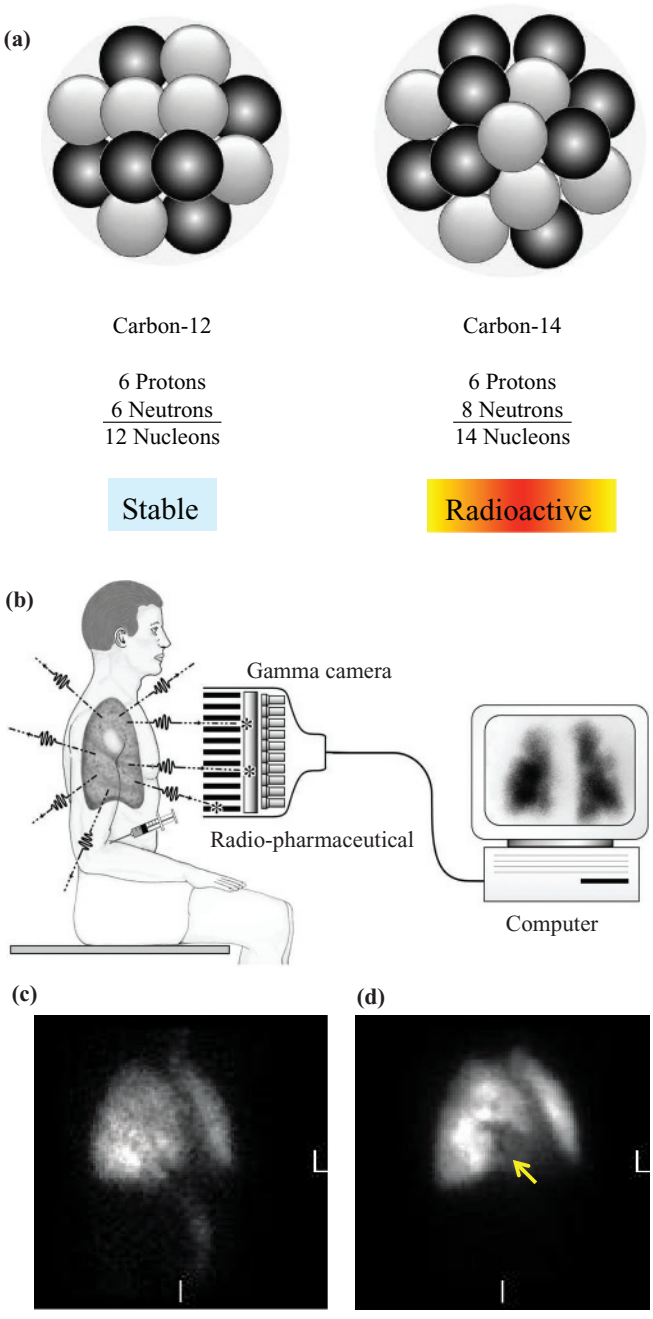

Figure 1.15 In a nuclear medicine examination, a specific radiopharmaceutical tracer is administered and taken up preferentially by a particular organ or other biological compartment, and from there it radiates gamma-rays. (**a**) The *element* type of an atom is determined solely by its *atomic number*, *Z*, which is the number of protons, hence the positive charge, in its nucleus. The various *isotopes* of a given element are atomic species that all have the same atomic number, but that differ in the number of uncharged, massive *neutrons* in the nucleus. The several isotopes of an element are virtually identical in their chemical, electrical, thermal, magnetic, and other normal properties, but they will differ radically in the behavior of their nuclei. The *radioisotopes* of an element, in particular, comprise a subgroup of its isotopes that are *radioactive*; that is, they undergo spontaneous nuclear transformations with the release of gamma-rays or positrons, or of other emissions that are *not* of interest in imaging. (**b**) Just as an ordinary camera creates photographs out of visible-light photons, a *gamma camera* produces images out of gamma-rays emitted by radionuclides concentrated in biological compartments within the body. (**c**) Normal ventilation and (**d**) irregular perfusion components of a (V/Q) study of the lungs in a patient presenting with acute, stabbing chest pain and shortness of breath, suspected of being associated with a pulmonary embolic event. This diagnosis is nearly confirmed when a perfusion mismatch is demonstrated by the wedge-shaped perfusion defect (arrow) in an area that is fully ventilated.

to interact with the image receptor (a large, fluorescent single crystal of sodium iodide, NaI); a half-life (6 hours) that allows preparation of the radiopharmaceutical and its uptake by an organ, but does not irradiate the patient or others too long after; and the ability to fasten resolutely to a wide range of inexpensive and convenient tissue-seeking chemophysical agents, which are readily available in kits.

Just as a red-hot poker glows in a dark room, a biological compartment containing radiopharmaceutical will "glow" gamma-rays. A *gamma camera* can detect and process them, just as an optical

camera captures visible-light pictures (Figure 1.15b), providing a powerful way to evaluate metabolic function of tissues. A gamma camera functions somewhat like an eye. Gamma-rays, unlike light, cannot easily be focused, however, so the role of the lens is played by a *collimator*, a 1 cm thick, highly attenuating lead plate honeycombed with closely-spaced parallel (or nearly parallel) open channels. Behind the collimator is a life-size, thin single, transparent fluorescent sodium iodide crystal. Any gamma-ray that passes straight along a channel of the collimator, and then interacts with the crystal, triggers the production of a *scintillation* (pinpoint burst of light). The crystal is viewed from the back by an *array* of up to a hundred small electronic photomultiplier tubes (PMT), light-sensitive detectors that are attached to a scintillation-location circuitry; together, these play the role of the retinal photoreceptors and neural network of the eye. The photodetector assembly senses each such event and determines its location within the crystal, which corresponds directly to the origin of the gamma-ray within the body, and displays it on the monitor.

Creating contrast through differential uptake of photon-generating radiopharmaceuticals

To summarize: nuclear medicine is based upon *differential uptake* of radiopharmaceutical by various tissues followed by a corresponding spatial *differential emission* of detectable gamma-ray probes.

With a typical *ventilation* (V) study of the lungs, inhaled radioactive xenon gas or aerosolized Tc-99m is evenly distributed throughout the airways to which it has access (Figure 1.15c). The portion of lung air-space containing the radioisotope will glow, with any dark regions revealing volumes where air flow is somehow impaired. No defect is noted in this right anterior oblique (RAO) projection, demonstrating homogeneous ventilation and uptake of the radiopharmaceutical.

In the accompanying *perfusion* (Q, meaning "flow") study, Tc-99m-labeled MAA is injected through a peripheral vein, after which it is briefly trapped within about 1% of the pulmonary capillaries. The radionuclide radiates gamma-rays, and any abnormally dark area may indicate a problem, such as a tumor, and associated regional blockage of blood flow. An area where a blockage exists is evident here, giving rise to a pyramidal defect of hypoperfusion (arrow) (Figure 1.15d). The two parts of this combined V/Q study display a "mismatched" defect, which, while perhaps not visible on a conventional chest X-ray, has a high diagnostic specificity for acute pulmonary embolism.

Nuclear medicine images are of relatively low spatial resolution, typically about 3–4 cm, and reveal only the location, size, and rough shape of the organ or tissue under consideration. But if a part of the organ fails to take up the radioactive material, or is missing, or is eclipsed by abnormal overlying tissues, then the corresponding region of the image will appear dark. Conversely, any part of the organ that takes up an excess of radiopharmaceutical will look unusually bright. So a nuclear medicine image provides information mainly on the physiological status of an organ, parts of which may be affected by a pathology, rather than on the fine details of its anatomy.

SPECT and PET

Just as CT solves the problem of overlapping images in radiography, so also does SPECT in nuclear medicine. In SPECT, several standard gamma-camera heads rotate slowly (∼20 minutes) about the patient (Figure 1.16a), and the accumulated data allow reconstruction of a set of CT-like slices that can either be viewed individually or combined to produce three-dimensional structures.

About half of all SPECT studies are ECG-gated cardiac stress tests for coronary artery disease, and a good fraction of the rest are for bone studies. Applications in oncology are expanding, with increasing numbers of agents becoming available for detection of specific tumor-types (Figures 1.16b). It is increasingly common practice to acquire the corresponding detailed anatomic data with CT or MRI (Figure 1.16c), and superimpose the images.

Photons attempting to exit the body may be absorbed or scattered by outer-lying tissues, of course, compromising the ability to obtain a precise map of differential emission; it is therefore practically essential, to be able to compensate for that effect by computing *attenuation corrections* for both SPECT and PET.

PET makes use of a few unusual and difficult-to-produce atomic nuclei that emit a *positron* (the

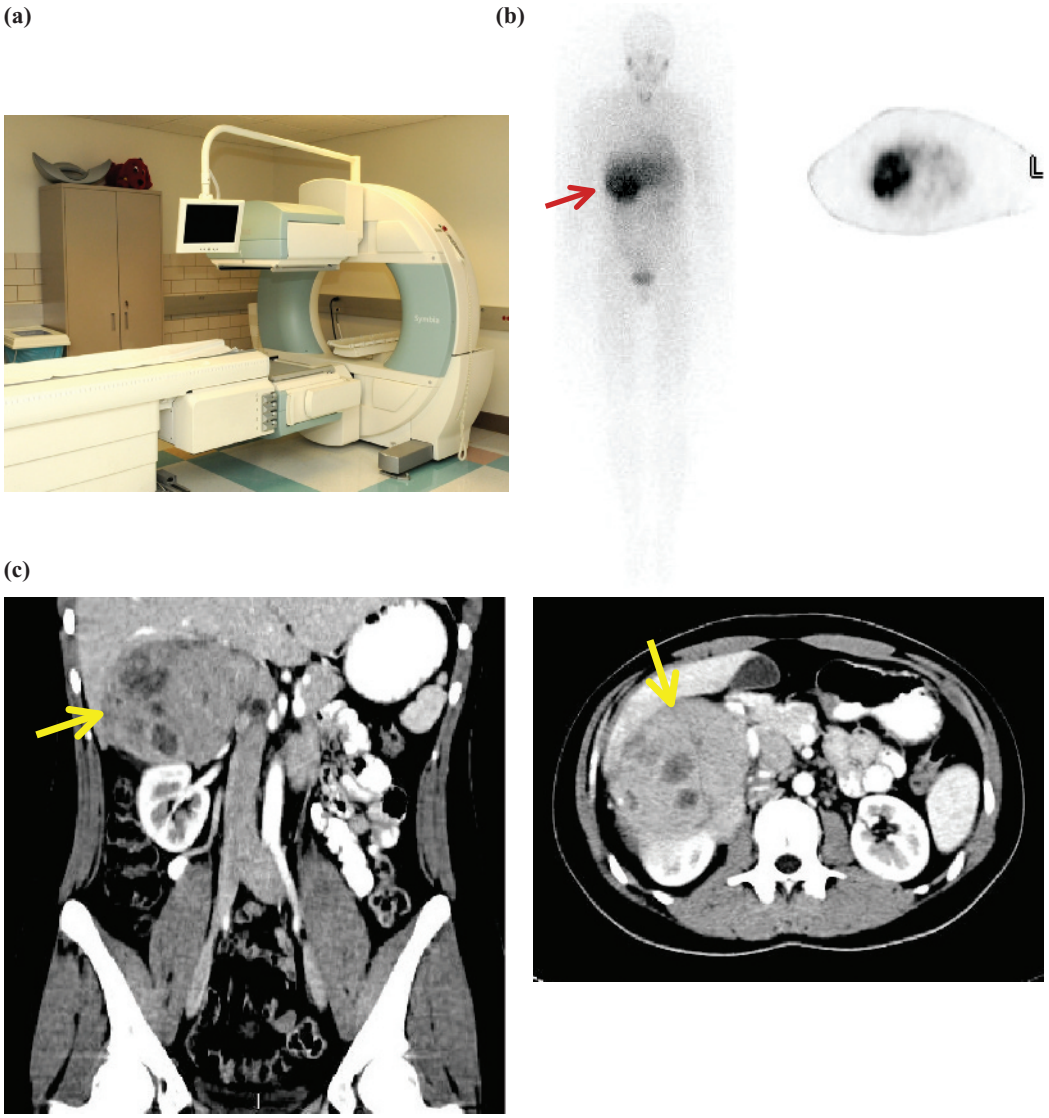

Figure 1.16 Single photon emission CT (SPECT). (**a**) A two-headed SPECT imager. Alternatively, either gamma camera head, or both together, can serve for a (faster) standard planar study. (**b**) Whole-body 3D scintigraphy with the agent metaiodobenzylguanidine (MIBG) labeled with iodine-123. MIBG resembles noradrenaline and is actively taken up by cells of neuroectodermic tumors. The "hot spot" of activity at the level of the right upper abdominal quadrant (arrow) in this patient with malignant hypertension is caused by a pheochromocytoma. The axial (transverse) SPECT reconstruction confirms the presence of this mass just caudal to the liver. (**c**) Contrast enhanced CT images in intersecting coronal and axial planes show the mass located at the level of the right adrenal gland, representing a pheochromocytoma (arrows).

positively charged antiparticle to the electron) in radioactive decay, rather than a gamma-ray. A positron travels a millimeter or so in tissue before colliding with an ordinary atomic electron, whereupon the two *annihilate* one another, transforming their masses into "pure energy" in the form of a pair of 511 keV *annihilation photons*. (By $E = mc^2$, the energy equivalent of the mass of an electron is 511 keV.) The two photons travel off in opposite directions at the speed of light (Figure 1.17a), and *coincident* (almost exactly simultaneous) detection of many such pairs allows localization of their

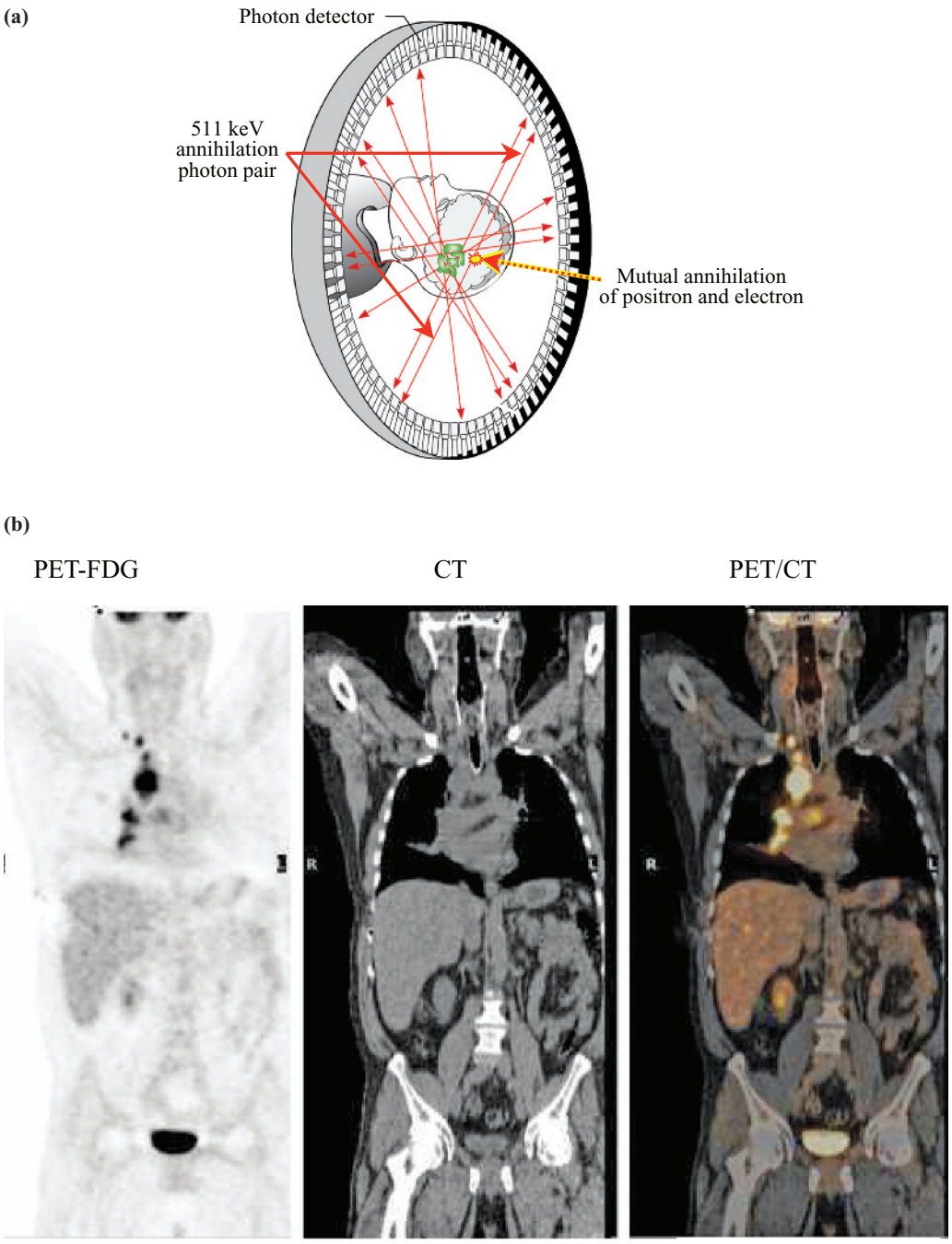

Figure 1.17 Positron emission tomography (PET). (**a**) The two *positron annihilation photons* trigger two detectors on opposite sides of the patient *in coincidence*; they originated at a point somewhere along the line between them, to within 1–2 mm. (**b**) To help with anatomic interpretation, PET information is commonly superimposed on a CT (or, still to a much lesser extent, an MRI) study of the same region. In this example, the PET image, to the left, displays foci of metabolic hyperactivity in right hilar and suprahilar masses, indicative of neoplasms. A conventional CT coronal view (re-created from a set of transverse slices) demonstrates the anatomic structures of the chest and abdomen. Superimposing these two and adding a color spectrum scaled to the relative number of positron events, hence to the metabolic activity, demonstrates and localizes the lesions. It also shows the normal metabolic activity within the liver and the absence of any other "hot spots." Courtesy of Robert Hellman, Medical College of Wisconsin, Milwaukee.

region of origin within the body; from that comes the image of the spatial distribution of the radiopharmaceutical in the body. (Any photons detected one at a time, rather than in pairs, are totally ignored.)

Some of the elements with positron-emitting isotopes (carbon-11, nitrogen-13, and oxygen-15) can be incorporated into physiologically important biomolecules. Most widely employed of these, by far, is the glucose analog fluorine-18 deoxyglucose (^{18}FDG), which tends to concentrate in tumors and other areas of high metabolic activity (Figure 1.17b). Virtually all PET imaging is now *multimodal*, in that the physiological contrast provided by the nuclear medicine study is superimposed on a background of anatomic landmarks obtained at about the same time with a CT machine that is either physically co-joined with the PET device, preferably, or separate from it. New PET devices come automatically with a CT attached.

PET studies are particularly intriguing to neuroscientists and psychiatrists, since ^{18}FDG may indicate the parts of the brain where neural activity becomes notably high when certain mental processes are ongoing. Dynamic PET studies provide information that is similar, but not identical, to those of *f*MRI, and the combination of these complementary modalities (and perhaps with others, such as electroencephalography and magnetoencephalography) shows great clinical potential in the fields of mental health.

Diagnostic ultrasound: contrast from differences in tissue elasticity or density

Unlike the other imaging technologies we have discussed, ultrasonography does not involve ionizing radiation. In fact, the probes involved are not EM radiation of any sort but, rather, high-frequency *mechanical* disturbances that travel through soft tissues in fairly straight lines and at almost constant velocity.

Normal audible sounds consist of waves of compression and rarefaction, of frequencies between 20 Hz and 20 kHz, that flow through air at about 343 m/s at sea level and room temperature. When a drum is struck, for example, its vibrating head alternately increases and reduces the pressure in the air just outside it, which pushes and pulls on the adjacent thin "layer" of air a brief moment later, and so on. The disturbance thus radiates outward as waves of mechanical energy, and a small part of it reaches the ear, driving displacements of the tympanic membrane, and leading to oscillations of the fluid in the cochlea. The actual sound receptors are hair cells within the organ of Corti, sensory neurons attached to microscopic stereocilia of various lengths and weights that resonate naturally over a range of frequencies, and they can be set in motion by vibrations in the cochlear fluid, triggering the cochlear nerve. The transmission of action potentials along the neurons of the eighth cranial nerve to the brain results in the sensation and perception of sound.

Ultrasound waves are similar, except that they are of frequencies far above the audible range, typically between 2 and 10 megahertz (MHz), and they propagate through soft tissues much faster (about 1540 m/s) than does sound in air.

B-mode anatomic imaging

A clinical ultrasound system used for medical diagnosis is similar to active sonar (*so*und *na*vigation *r*anging), developed largely during the Second World War for the detection of submarines. The heart of a US system is the *transducer*, an energy-conversion device that transforms pulses of electrical voltage into mechanical vibrations, and vice versa. The transducer is pressed against the body and, acting somewhat as an audio speaker, produces a narrow, focused beam of pulses of US. In a homogeneous material, such as water or the fluid contents of a cyst, the beam simply dissipates its energy as it penetrates to greater depths, somewhat analogous to the attenuation of a monochromatic beam of X-rays passing through a homogeneous medium. But if a beam passes from one tissue into another, energy is also reflected back at the interface between them (Figure 1.18a).

By analogy, imagine a pair of joined springs of different mass per length or elasticity (Figure 1.18b). When a pulse moving along from one end encounters the junction, some of its energy will continue in the forward direction but the rest will be reflected back as an echo; in an extreme case, with the spring attached to a wall, virtually the entire pulse will be reflected, but returned upside-down. This

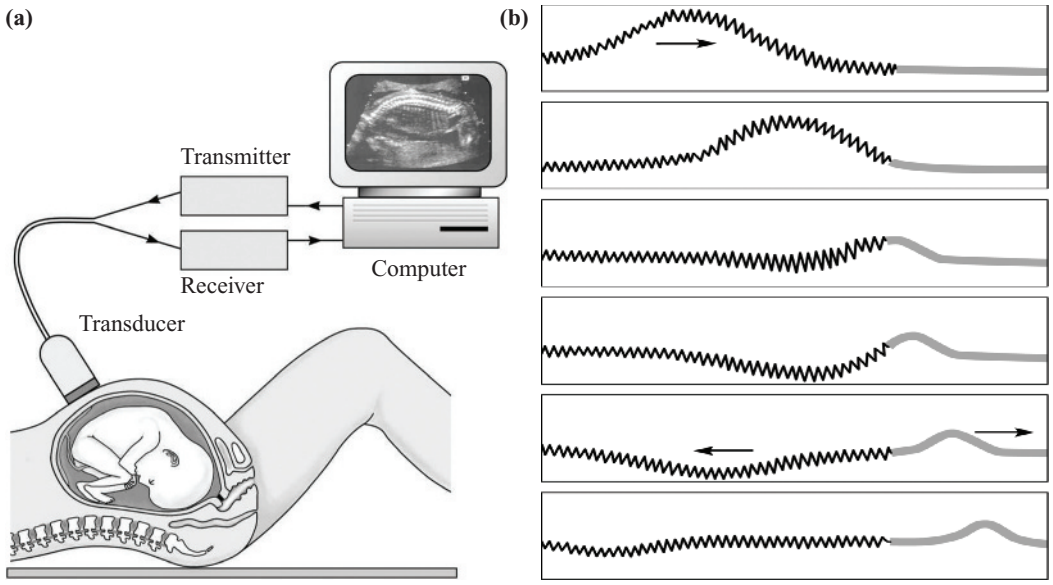

Figure 1.18 Ultrasound imaging. (**a**) Under the control of a computer, electrical pulses from the transmitter, typically 1 per millisecond, are transformed into a narrow, brief beam of high-frequency (2–10 MHz) sound by the transducer. Then, acting in reverse after each pulse, the transducer detects echo signals produced at tissue boundaries and converts them back into electrical signals. Meanwhile, the beam is swept or stepped relatively slowly (30 times per second) across the body, cutting out a thin plane. The computer then untangles all the echoes and creates an image. (**b**) Echoes arise when US encounters a boundary between tissues of significantly different density or elasticity, much as when a pulse traveling along a spring is partly reflected at a juncture with a different type of spring.

figure is a little misleading, however, in that the displacements of the spring are shown as transverse to the direction of wave propagation; with sound and ultrasound, they are longitudinal, vibrating back and forth along the direction the waves are moving.

After reflection at inter-tissue boundaries, the US echoes are detected by the transducer, now serving as a microphone, and transformed back into electrical signals. The *time of return* of an echo is proportional to the *depth* within the patient of the interface that produced it. The echo's *intensity* depends on the degree of difference in *density* and/or *elasticity* of the materials on the two sides of the interface, as well as on its depth.

Ultrasound is most useful in the study of soft tissues and organs that are radiologically too similar to provide adequate X-ray image contrast, as in Figure 1.19. It is widely used for obstetric/gynecologic, cardiac, and general abdominal imaging. B-mode can assist in diagnosing a wide range of diseases, like pathological changes in the thyroid, gall bladder, pancreas, kidneys, and heart, and in distinguishing a fluid-filled cyst from a solid neoplasm in the breast or abdomen. Dependent upon the condition being evaluated and the skill of the observer, it can achieve a high degree of clinical precision. US evaluation of an ovarian cystic mass is more diagnostic than direct observation via laparoscopic or open surgical evaluations in some situations, such as if it is inappropriate to take a biopsy specimen. It may also disclose more soft tissue detail than CT, as well as being much faster and less expensive. Ultrasound serves as a guide in carrying out invasive procedures such as the draining of an abscess or other fluid collections, or in approaching a vessel to obtain vascular access. US energy does not pass readily across tissue/air or tissue/bone interfaces, however, and is therefore of limited use for the study of the lung or of the adult cranial cavity.

Doppler imaging of blood flow

A quite different form of US allows the monitoring of blood flow. Wave signals coming from a moving source or detected by a moving observer may be shifted in pitch by an amount proportional to their relative speed and direction, as is evident in the wail

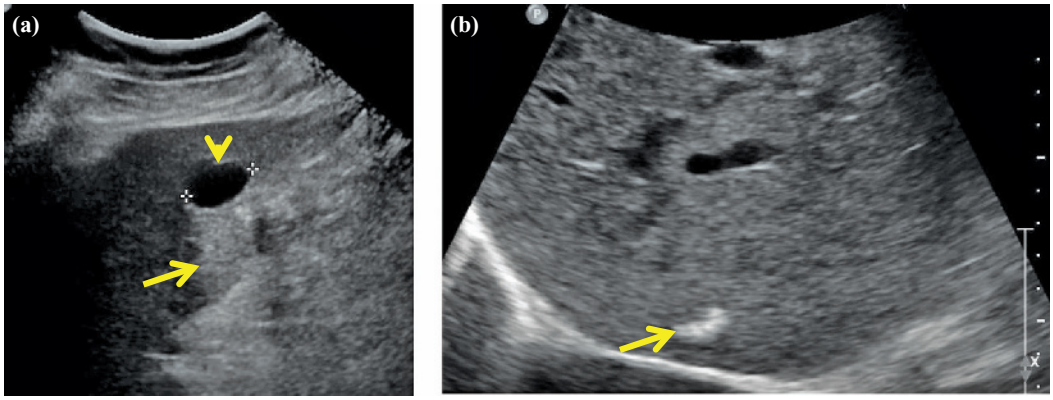

Figure 1.19 In certain situations, the overall US appearance of a lesion can be pathognomonic, characteristic of a specific problem, in which case no further imaging is required. (**a**) Liver with a simple cyst. In the absence of any intrinsic tissue interfaces, the fluid within the cyst transmits the sound waves anechoically, giving the lesion a black appearance (arrowhead). Because little energy was attenuated and removed from the beam within the cyst, the tissues beyond it are brighter than normal, and that part of the image is said to be "enhanced" (arrow). (**b**) US image of a liver containing a hyperechoic rounded lesion, typical of a benign hemangioma (arrow).

of the siren of a fire truck rushing by. That is also the basis for the red-shift determination of stellar velocities, police Doppler radar, and the Doppler ultrasound measurement of blood flow within larger vessels: the faster the blood cells are traveling, the greater the shift in the frequency of the US waves that bounce off them and return to the transducer (Figure 1.20).

It is commonly held that there is virtually no risk to a patient from ultrasound, since no ionizing radiation is involved. At diagnostic intensities, there are no known harmful biologic effects, even to a fetus; this is one reason the modality is used extensively to provide obstetric information and as a visual aid in guiding amniocentesis and fetal surgery. But absence of evidence of health effects from US is not certain evidence for their absence, and one should treat this modality (and all others) with due respect. Indeed, high-intensity US is destructive of tissues, and such beams are used therapeutically to ablate abnormal tissues, or to disrupt crystalline structures such as with nephrolithotripsy. So it is important always to ensure that diagnostic equipment is functioning properly, being operated correctly, and being applied for a medically valid reason, especially when used on the fetus.

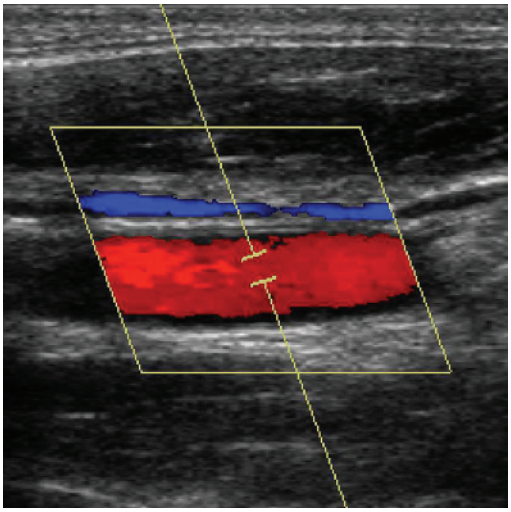

Figure 1.20 In this Doppler image, the red and blue regions indicate blood moving toward and away from the transducer, respectively.

Magnetic resonance imaging: mapping the spatial distribution of spin-relaxation times of hydrogen nuclei in tissue water and lipids

We have already discussed creating contrast through the attenuation of X-rays, the emission of gamma-rays, and the reflections of ultrasound waves. MRI produces contrast in a number of distinct and far more subtle ways, and at times it can provide information on soft tissues that is much more diagnostically useful than the others.

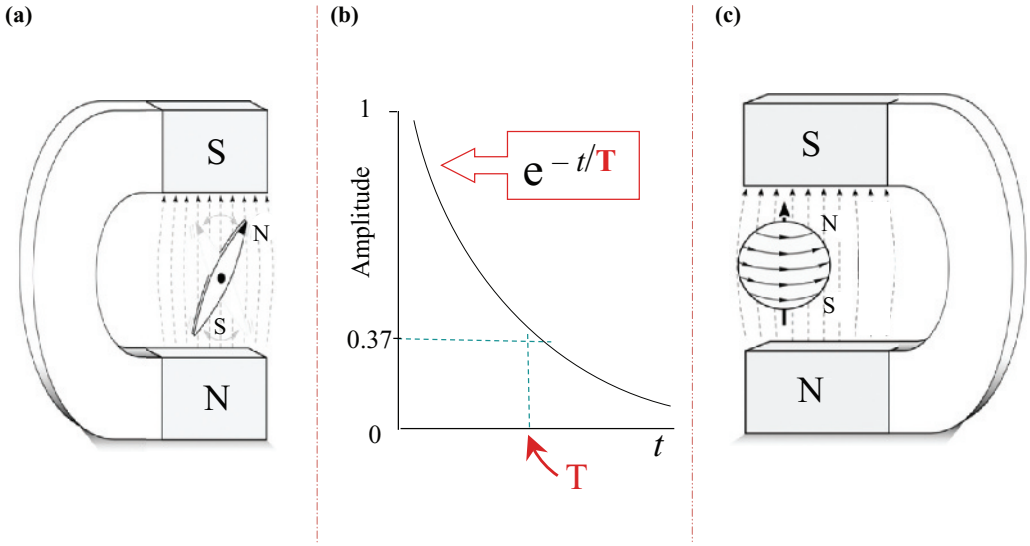

Figure 1.21 The NMR process, central to MRI, can be viewed in several ways. **(a)** With one, spin-relaxation is *analogous* (only!) to the settling down of the swings of a briefly jostled compass needle in a magnetic field, **(b)** with a characteristic *relaxation time*, here called T. **(c)** Like any moving charge, a "spinning" lone proton, the nucleus of a standard hydrogen atom, creates a tiny magnetic field, like that of a compass needle; during NMR, it, too, undergoes a subtle sort of relaxation, but we shall have to provide a good deal more background information to explain it.

MRI not only reveals the structural, anatomic details of the various organs, like CT, but it can also provide information on their physiological status and pathologies, like nuclear medicine. And as with US, there is no risk from ionizing radiation to the patient or staff, since no X-ray or gamma-ray energy is involved. Instead, MRI harnesses magnetic fields and radio waves to probe the protons — in particular, the nuclei of the ordinary hydrogen atoms occurring naturally in water and lipid molecules, within and around cells.

Spin-relaxation times of protons in water and lipids in a strong magnetic field

Imagine a bunch of identical pocket compasses on a table. Each compass needle is itself a tiny bar magnet, and as such it displays two related but different characteristics: it produces its own small magnetic field, and also it tends to align along the Earth's magnetic field.

In your mind's eye, twist all the compasses through 180°, so that they point south, and then release them at the same time (Figure 1.21a). Each will flop back over again, oscillating about north, with an amplitude that diminishes exponentially over time – eventually they all come to rest pointing north again (Figure 1.21b). The length of time this settling down process takes, as averaged over all the compass needles, is parameterized by their average *relaxation time*, T. For a compass, T is determined largely by the mass and shape of the needles, the nature of the frictional forces such as those occurring at the mechanical pivot points where the needle is supported, and the viscosity of any damping fluid that might surround it.

For protons in water and lipid molecules in tissue, relaxation is a somewhat *analogous* affair, but far more nuanced, interesting, and clinically useful. But first . . .

Fact of life: any electric current gives rise to a magnetic field. If you hold one of our compasses close to a wire that connects a battery to a flashlight bulb, the needle will deflect. It's one of the fundamental wonders that underlie the physical sciences, like the electrical force between charges or gravitational attraction. Physicists can fancy it up, what with descriptions involving quantum mechanics and relativity, but it really doesn't get any more basic.

A proton, the nucleus of a hydrogen atom, behaves somewhat like a rapidly spinning, hence moving, positively charged ball. So it, too, produces its own small magnetic field along its spin axis and, as such, it acts like a tiny compass needle

(Figure 1.21c). In particular, when a patient lies in the extremely strong magnetic field of an MRI device (typically of strength 1.5 *tesla*, some four orders of magnitude (10^4) times greater than the Earth's field), many of the protons in tissue water and lipid molecules will tend to align along it.

It is possible, by beaming in a brief pulse of radio waves of the correct frequency, to make protons in a voxel flip over and point in the opposite (i.e., the "wrong") direction, instead. Immediately thereafter, though, some of these will begin a kind of spontaneous relaxation in which they return to their more comfortable, equilibrium alignment *along* the field. This transition takes place in a manner analogous to (but, on the molecular scale, quite different from) that of a compass needle. The rapidity of the relaxation process for the protons in the voxel is parameterized by its characteristic *nuclear spin relaxation time* known, in MRI, as T1.

The rates of relaxation of excited water or lipid protons within and between cells are exquisitely sensitive to the detailed nature of the local biochemical environments of the protons involved – that is, to the atomic-level friction-like and other physical interactions between them and the nearby biomolecules. The concentrations and biophysical characteristics of these biomolecules, in turn, depend on the type and physiologic status of the tissues, and that will influence the effectiveness of the T1 relaxation mechanism for them. A spatial map of T1 throughout a slice of tissue can therefore produce clinically invaluable anatomic and/or physiologic information.

There is a second sort of proton relaxation process, known as T2, that involves and reflects on quite dissimilar aspects of molecular biophysics, and T2-maps also play a central, and complementary, role in MRI. Indeed, MRI can produce contrast by way of half a dozen totally different physical processes, with countless variations on each theme, and they can all provide useful clinical information.

Mapping the spatial distribution of proton T1 and T2

What MR imaging usually does, then, is to produce a map of variations in the relaxation times of the hydrogen nuclei in the water molecules, primarily, of the tissues (Figure 1.22). T1 or T2 contrast among soft tissues is often much better than that from imaging with X-rays, and it can show subtleties in the physiology of an organ that CT would completely miss. In addition, some forms of MR imaging have no counterparts in other forms of imaging. As seen in the introductory case of Dr. Doe, *f*MRI monitors stimulus-induced local changes in cerebral blood flow and, like PET, can indicate the occurrence of mental processes (Figure 0.5). DTI makes it possible to follow the natural diffusion of water molecules along the axons of neurons, thereby revealing nerve-trunks (Figure 0.6). One can carry out *in vivo* biopsy studies on small volumes of tissue with MR spectroscopy (MRS) (Figures 0.4). It even supports several approaches to MR angiography (MRA) that are non-invasive and do not necessarily involve contrast agent (Figure 1.23).

MRI came onto the scene in the early 1980s, and at first data acquisition was slow, requiring an hour or so per patient. Imaging time has been driven down dramatically and is becoming much less of a major limiting factor; indeed, imaging of the heart throughout the entire cardiac cycle is now routine. Similarly, resolution has improved steadily, and is now better than 1 mm.

MRI is widely and appropriately touted for the absence of ionizing radiation, and it appears that the various strong constant and time-varying magnetic fields involved pose no deleterious physiological effects. Still, one must be ever vigilant for magnetic shrapnel and implants (such as aneurism clips and pacemakers) and for flying screw drivers, oxygen bottles, i.v. poles, hand-cuffs, and the like).

Hopefully these brief sketches have whetted your appetite for a deeper understanding of imaging technologies.

Traditional X-ray filming is still the form of imaging most commonly employed worldwide, and the least expensive. It's also the easiest to describe so, after briefly exploring what a "good enough" medical image means in the next chapter, we shall start off our more in-depth examinations with a reconsideration of radiography.

Appendix: selection of imaging modalities to assist in medical diagnosis

The following is a *sampling* of examples of the selection of common imaging studies of major biological

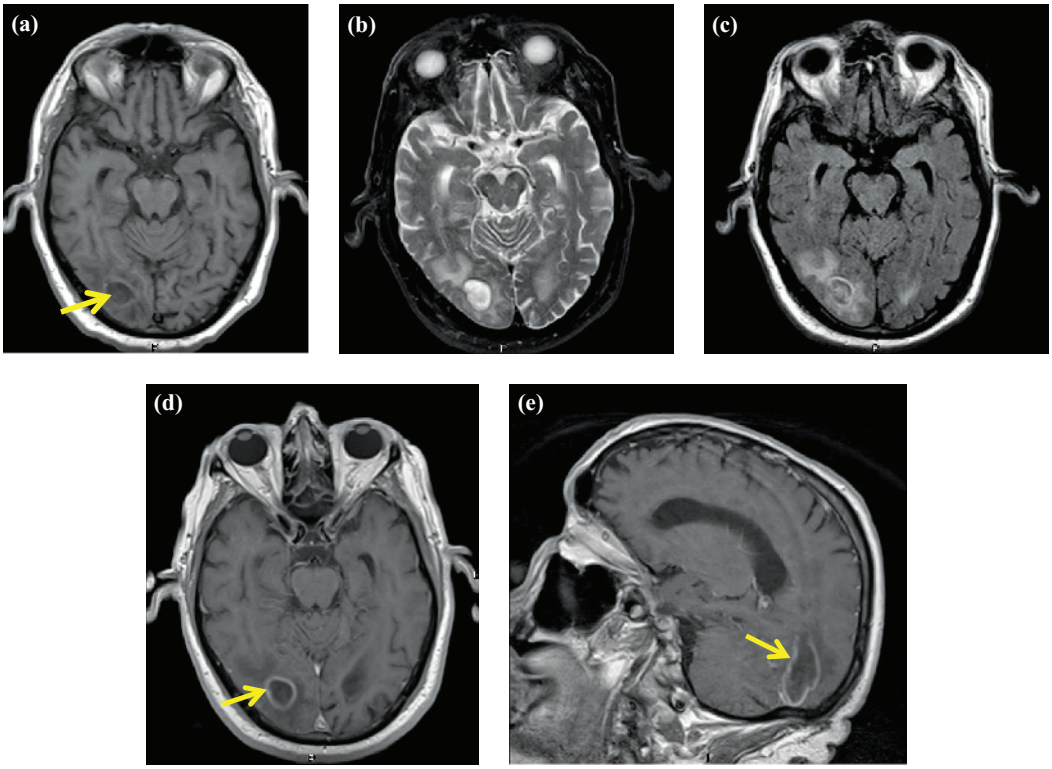

Figure 1.22 A patient known to suffer from AIDS presents with mental status changes, and (**a**) an initial axial T1-weighted acquisition demonstrates a hypointense, well-circumscribed lesion of the white matter of the right occipital lobe (arrow). The lesion has an isointense rim and is surrounded by hypointense edema. *Note*: One views a transverse/axial tomographic slice-image from the feet upward; the arrow, to the reader's left, is on the patient's right side. (**b**) Axial T2-weighted image at the same level further categorizing the lesion and demonstrating the surrounding edema. (**c**) Axial fluid attenuating inversion recovery (FLAIR) study at the same level, for which the cerebrospinal fluid is dark while the perilesional edema is hyperintense. (**d**) With the intravenous addition of contrast agent (a gadolinium complex), a repeated axial T1-weighted image demonstrates circumferential ring enhancement of the wall of the lesion still surrounded by hypointense edema (arrow). (**e**) This is also demonstrated clearly in an image of a thin sagittal plane through the center of the lesion, where it is seen to be located above the tentorium cerebella (arrow). The overall appearance and contrast enhancement pattern is typical of an abscess and, because of the patient's immunosuppression, the infection was likely to due to *Toxopolasma gondii* (as was proven by biopsy).

systems of the body, based on typical symptoms. It is meant only to provide a few illustrations of possible studies and the order in which they might be chosen, as determined by factors such as diagnostic sensitivity and selectivity. For all the following, diagnostic benefit must be weighed thoughtfully against considerations of safety (especially of the fetus and children), cost, and normal availability of the equipment. Estimated relative cost is indicated by $, $$, and $$$, and dose of ionizing radiation by *D*, *DD*, and *DDD*.

The objective of this appendix is only to illustrate some conventional clinical applications of the modalities discussed in the book. This is obviously very far from complete, and it reflects the opinions of two physicians. It is not intended to serve as medical advice, nor should it be construed as such.

Cardiac versus non-cardiac chest pain

Chest pain presents in two broad categories based on symptomatology and ancillary testing (EKG, cardiac biomarkers, etc.): *cardiogenic* and *non-cardiogenic*.

Cardiogenic chest pain: acute coronary syndrome (ACS) typically presents as:

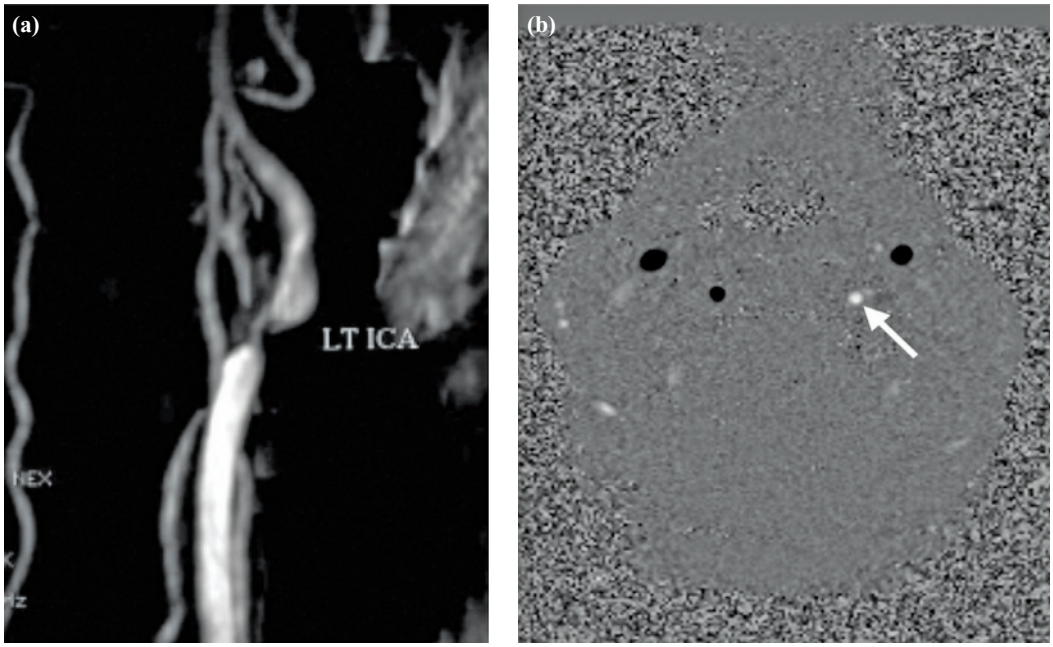

Figure 1.23 Magnetic resonance angiography. (**a**) Contrast agent (gadolinium) enhanced MRA 3D image demonstrating a stenosis of the left interior carotid artery. After a disruption, protons in most of a thin horizontal slice of soft tissue recover according to relaxation times T1 and T2; with Time of Flight (TOF) MRA, blood within the voxels of a vessel within the slice, however, is refreshed with the inflow of new blood, and spin-change within them is governed primarily by the rate of flow. (**b**) Phase contrast (PC) MRA differs in that it indicates the direction of flow, as well as the rate. Flow in the left vertebral artery is normally in the caudal-to-cranial direction, and shows up dark; at the arrow, it is bright, indicating retrograde flow, resulting from *subclavian steal*.

Chest pressure (not necessarily sharp pain) with radiation to left shoulder, left arm, left side of neck or jaw;

Associated symptoms of dyspnea and/or nausea and vomiting;

EKG findings of ST-segment elevation corresponding to area of infarct, or ST-segment depression indicating evolving myocardial ischemia;

Elevated biomarkers (troponin-i, creatine kinase-MB (CK-MB), myoglobin) in serum.

Presentation with the classic findings of cardiogenic pain is typically treated with nitroglycerin and thrombolytics, or the patient goes directly to the cardiac catheterization lab for evaluation of coronary anatomy with possible intervention, such as percutaneous thrombolytic coronary angiography (PTCA). Patients with somewhat equivocal findings of cardiogenic type chest pain, however, may benefit from other (less invasive) imaging modalities to determine the etiology of their pain.

Non-cardiogenic chest pain lacks features clinically to be of a likely cardiac source, and therefore follows a different path of investigation. This class of imaging is outlined below for patients who present with chest symptoms (sharp chest pain, isolated dyspnea, chest trauma or mass).

Non-cardiogenic chest pain

Atypical chest pain, dyspnea or chest mass, clinically thought to be not of cardiac origin: imaging the chest in patients with "non-cardiogenic" chest disease typically coalesces around the symptoms or findings of atypical chest pain (sharp, pleuritic, worse with deep breathing), mass, chest trauma, dyspnea or hemoptysis. Diagnoses range from minor to life-threatening (bronchitis to pulmonary embolus).

Chest radiographs (CXR), PA and lateral ($; D): Visualization of pleural membrane and space, lung disease (pneumonia, pneumonitis, interstitial lung disease, atelectasis) mediastinal mass/adenopathy, aortic dissection, cardiomyopathy, lung mass, pulmonary edema, pleural effusion, pneumothorax, pneumoperitoneum, hemothorax, rib fractures, ET tube placement, diaphragmatic integrity, stomach

gas, or foreign body. Poor discrimination of hilar versus mediastinal adenopathy or mass; poor sensitivity for evaluation of PE.

Chest CT ($$; DD): Greatly improved sensitivity, specificity, and discrimination of/for: hilar and mediastinal mass; pulmonary disease, pleural disease, and chest wall; staging lung cancer and imaging of lung/pleural mass; cardiac anatomy visualization; chest trauma (tracheal rupture, aortic dissection, pneumomediastinum), pleural/lung disease versus mass, lung abscess versus nodule, interstitial versus infiltrative pulmonary processes. In patients with infectious pulmonary disease, lung abscess versus empyema, rapid evaluation of chest trauma, percutaneous drainage.

Chest CT for PE ($$$; DDD): Suspicion for pulmonary embolus or deep vein thrombosis (DVT) with dyspnea. Requires timely specific IV contrast, minimum 20 gauge, for vascular visualization. 95% sensitive for clinically significant PE.

Chest MRI ($$$; No D): No ionizing radiation: better lung mass characterization and cancer staging, visualization of aorta and mediastinum; discrimination for mediastinal versus hilar mass/adenopathy, vascular invasion in hilum or mediastinum, interstitial versus infiltrative pulmonary disease; congenital heart disease or cardiac tumor. Contraindicated in patients with most pacemakers, intraocular metal, metal clips, cochlear implants, kidney disease (see Box 11.5).

V/Q scan ($$; DD): Evaluation of functional ventilation for dead space, perfusion for shunt. Most scans are intermediate probability for PE, which leads to diagnostic dilemma (20–70% accuracy) giving low specificity for thromboembolic disease. High- and low-probability scans are of excellent sensitivity and specificity.

Chest PET/CT ($$$; DD): Tumor staging for pulmonary or mediastinal, primary or metastatic malignancy. Discriminates benign and malignant mediastinal adenopathy. Metabolic and anatomic information

Cardiogenic chest pain

Chest pain of typical cardiac origin: Substernal pressure with radiation to the left shoulder, jaw, or arm. Although any chest pain or dyspnea (angina equivalent) can be of a cardiac origin, suspicion for ACS is raised when pain posterior to sternum is of a typical cardiac nature.

Chest pain of an atypical nature: With equivocal cardiac testing, such as EKG findings suspicious but not confirmatory of ACS. Imaging in these equivocal cases of borderline historical chest pain associated with other clinical signs and findings potentially consistent with coronary occlusion, coronary artery disease (CAD) involve both cardiogenic and non-cardiogenic imaging strategies. The chest radiograph is the starting point for addressing both types of chest pain or dyspnea. Beyond that, clinical judgment directs testing and imaging.

Myocardial perfusion stress, technetium, thallium ($$$; DD): Typical cardiac pain, atypical chest pain with known ACS, extent of myocardial ischemia. Detection of presence, location, and extent of active ACS/ischemia. Stuttering course of chest pain with uncertain diagnosis; chest pain with equivocal EKG changes and negative cardiac biomarkers; atypical or recurrent chest pain of uncertain etiology.

CT coronary angiography ($$$; DD): Chest pain suggestive of ACS, equivocal EKG changes, negative cardiac biomarkers. Consider direct correlation of observed angiographic stenosis (CAD) with symptoms of coronary lesions. Similar limitation observed with coronary angiography.

Cardiac CT for calcium scoring ($$; D to DD): screening exam for patient with family history, multiple risk factors for ACS, or vague symptoms of possible coronary disease. High score suggestive of coronary stenosis.

Radionuclide ventriculography ($$$; DD): Multigated acquisition (MUGA). Patients with ischemic heart disease and congestive heart failure or cardiomyopathy. Calculation of ejection fraction. To evaluate cardiac output, ejection fraction is determined non-invasively. Difficult to perform if patient has abnormal rhythm.

Abdominal/pelvis imaging

The diagnostic and radiographic therapeutic work-up involving abdominal imaging is vast. Abdominal imaging and intervention typically clusters around the symptoms of abdominal pain (sometimes in quadrants) or diffuse abdominal or pelvic pain, abdominal mass/tumor, or vasculopathy (GI bleeding, ischemia, or vasculitis).

Abdominal radiograph ($; D): Screening for abdominal pain, need flat and upright views. Bowel gas pattern for mechanical small bowel obstruction versus ileus; pneumoperitoneum from

ruptured viscus or radio-opaque stone (urolithiasis, appendicolith, gallstones). Provides limited contrast.

Abdominal ultrasound ($$; No D): Cystic versus solid lesions of solid organs: hepatic or renal mass/cyst; biliary duct ectasia, cholelithiasis or gallbladder wall thickening; peri-pancreatic fluid of pseudocyst formation; hydronephrosis, hydroureter, abdominal aortic aneurysm, appendiceal inflammation, ascities, or metastatic or primary carcinoma (carcinomatosis). Visualization of pelvic masses, cysts and discrimination from GI source; pelvic masses are best visualized by US (complexity, architecture, thickness of wall). Can guide percutaneous drainage. Best results after 6 hours of NPO. Non-invasive and portable. Bowel gas can obscure; strongly operator-skill dependent.

Abdominal CT ($$; DD for non-contrast study; $$$; DDD for contrast-enchanced multi-phase study: All abdominal and pelvic organs. Small, large bowel obstructions; traumatic injury of any soft tissue organ, abdominal wall mass of injury (hernia); mass, tumor, cyst, or abscess evaluation; obstructive biliary disease, intra-hepatic process; pancreatitis or soft tissue inflammation. Visualization of mesenteric or retro-peritoneal adenopathy or mass. Appendicitis, mesenteric ischemia, urolithiasis or renal obstructive process. Abdominal aortic aneurysm. Uterine or ovarian mass and cancer staging of malignant disease.

IV contrast: Mesenteric ischemia or infarct, aorta, vascular enhancement of solid tumor.

Oral contrast: Rapid increased sensitivity of bowel wall. Excellent spatial resolution not limited by overlying bowel patterns. CT guided drainage or percutaneous biopsy may be possible. Contrast-induced nephropathy.

Abdominal MRI ($$$; No D): Adjunct to CT where superb resolution, tissue contrast, multiplanar views needed; benign versus malignant tumors, mass/tumor such as hepatic, bowel wall, or retroperitoneal. Pre-op staging of abdominal cancers. Subject to motion artifacts, may require IM-glucagon to calm peristalsis; opacification of GI tract not readily available.

Abdominal PET/CT ($$$; DD): Both metabolic and anatomic detail. Primary and metastatic neoplasms; benign versus malignant lymph nodes; tumor staging, evaluating recurrence.

Mesenteric angiography ($$$; DDD): Small bowel bleeding or mesenteric ischemia can be difficult to isolate by endoscopy or CT alone. For gastrointestinal hemorrhage not amenable to endoscopic evaluation/management; mesenteric aneurysm; vasculitis of splanchnic vasculature; embolization of acute GI-bleeding. Requires femoral artery cannulation and iodinated contrast, maybe sedation.

Radioniclide tagged labeled red-cell ($$$; DD): For slower rates (0.10 mL/min) of upper or lower GI bleeding, intermittent bleeding.

Upper GI fluoroscopy ($$; DD): Gastric and duodenal mucosal inflammation, ulcerations, polyps, mass, hernia, gastric outlet obstruction. Double or single contrast barium technique or gastrografin, water soluble contrast to check for anastomotic leak or perforation. Less expensive/invasive than endoscopy. But lesion identification may not correlate with site of bleeding or pain; barium may hinder subsequent endoscopic procedure, pulmonary edema from aspiration of gastrografin.

Radionuclide gastric emptying ($$$; DD): Functional information about gastric outlet not available by other means. "Dumping syndrome," gastroporesis, inflammatory or neoplastic processes. Establish normal values prior; patient must eat 300 gram meal of liquids and solids.

Radionuclide GI esophageal reflux ($$$; DD): Radionuclide scan evaluates gastro-esophageal reflux disease (GERD) or aspiration pneumonitis. Non-invasive and highly sensitive for GERD, quantification of reflux. But incomplete emptying may mimic GERD.

Radionuclide cholescintigraphy or HIDA scan ($$$; DD): RUQ, excretion of radionuclide into biliary system (biliary ducts, gallbladder, cystic duct, common duct, intestine) with hepatobiliary iminodiacetic acid labeled with technetium-99m (HIDA-Tc-99m). Hepatobiliary system function for suspected cholecystitis, common bile duct obstruction or bile leaks. 95% sensitive and 99% specific for cholecystitis (higher than ultrasound). But does not discriminate obstruction between tumor and stone.

Hepatic angiography {$$$; DDD): Gold standard for hepatic arterial anatomy, hepatic neoplasm. Liver trauma, arteriovenous malformation (AVM),

portal vein occlusion. Prior to TIPS procedure for portal hypertension, hepatic transplant. More specific than US for portal vein patency. But requires common femoral artery cannulation for contrast and cardiac monitoring.

Abdominal calcifications: non-palpable but seen on radiograph

Right upper quadrant: Cholelithiasis, renal mass with calcific degeneration, adrenal mass.

Left upper quadrant: Splenic artery calcification or calcified aneurysm, splenic mass or cyst, renal mass or pancreatic tail calcification.

Right/left flank: Urolithiasis and ureteral calculi or calcified mesenteric lymphadenopathy.

Mid-abdomen: Aortic aneurysm or calcified aorta, pancreatic mass, or metastatic lymph node.

Right lower quadrant: Appendolith or distal ureter stone.

Left lower quadrant: Ovarian dermoid, phleboliths, distal ureter calculus.

Pelvis: Uterine fibroids, bladder calculus, ureterovesicular junction stone, ovarian tumor, iliac vessels.

Head and neck imaging

Imaging of the skull, brain, sinuses for CNS infections, headache/trauma, mass, seizure, symptoms of dementia, acute delirium. Other changes in mental status are complex, commonly calling for: plain radiography, CT, MRI, angiography, and PET.

Radiograph: skull, sinus ($; D to DD): Cranial, facial bone fractures; nasal bone, orbital (blowout), Le Fort, mandible fractures, air-fluid levels in sinus. Skull fracture, linear or depressed. Osteomyelitis, several weeks after the process, with areas of lucency. Some tumors (chordoma) may reveal bony destruction or cortical expansion. Mucosal thickening or air-fluid levels in infected sinus.

Head CT – no contrast ($$; D to DD): Initial evaluation of trauma may reveal skull or facial fracture also showing soft tissue injury. Intra-cranial complications: epidural hematoma (convex peripheral high density lesion), subdural hematoma (crescent dense lesion), intracerebral hematoma, subarachnoid hemorrhage, or cranial contusion. A stroke/cerebrovascular accident (CVA) may produce a hypodensity involving a vascular territory in thrombotic CVA, or may be negative in early phases. Intraparenchymal hemorrhage appears as homogeneous dense, defined lesion within cerebral substance. Work-up for headache or possible brain mass may reveal a single heterogeneous mass which may be either isodense or hypodense (as in glioma). Infectious etiology such as meningitis (thrombosis, hydrocephalus, subdural effusion or brain abscess), encephalitis (low-attenuation) or epidural empyema can be visualized. Although non-contrasted head CT may be the first line to evaluate head trauma (acute bleeding and fracture), or CVA (to rule out hemorrhage), IV contrast may help for enhancement of mass, abscess.

Head CT – contrast enhanced ($$$; DD): Contrast enhancement may reveal necrotic tumor core with high-attenuation capsule, differentiates abscess versus tumor, tumor detail (homogeneous lesion with enhanced ring); vascular lesions, such as AVM.

Head MRI ($$$; No D): High T1-/T2-weighted tissue contrast. For neoplasms, image density (darkness) depends on tumor type: T2-*w* images show high density (dark) regions, but T1-*w* isodense (as in glioma). Acute hemorrhage of subarachnoid bleed will show on FLAIR as hyper dense signal. Alzheimer's dementia on MRI similar to CT, with cerebral atrophy and enlarged ventricles. Cerebellar atrophy, multiple sclerosis, seizure disorders, and/or encephalitis all may be best imaged with MRI; likewise with brain abscess versus necrotic tumor. In meningitis, inflammation of the two innermost layers of meninges, versus subarachnoid distention, as well as the etiology of hydrocephalus, are also best seen with MRI. When evaluating thrombotic CVA (after bleed is ruled out by CT), MRI T2-*w* image produces high signal intensity of vascular territory involved.

Duplex color-flow Doppler ($ to $$; No D): Hemodynamic information such as flow velocity for patients with transient ischemic attack (TIA) or CVA.

PET ($$$; DD): Functional pathology of neurodegenerative diseases: Alzheimer's, Parkinson's and Huntington's.

Musculoskeletal imaging

Radiography – extremity or spinal ($; D): Traumatic injury, musculoskeletal pain – typically adequate for uncomplicated fractures, dislocations of bones, joints in appendicular and spinal skeleton. For soft tissue (joint space, muscle) or when

sensitivity and specificity not adequate for musculoskeletal pathology.

Radionuclide bone scan ($$$; DD): Whole body evaluation of trauma (occult fracture), primary or metastatic neoplasm, osteomyelitis, arthritis, avascular necrosis, or joint prosthesis. Highly sensitive for osteomyelitis (early), stress fractures.

Bone/joint MRI ($$$; No D): Soft tissue in joint space and bone, except at prostheses; spinal nerve roots, cord, and vertebrae. Primary or metastatic mass involving bone or soft tissue. Soft tissue infections (abscess), marrow disease, or traumatic injury not visualized on plain radiograph or CT. CT may be superior in limited circumstances, such as osteophyte spurring.

Vascular imaging

Vascular imaging for venous thrombosis or patency; arterial stenosis, aneurysm or vasculitis leading to ischemia of a limb or organ system.

Ultrasound ($ to $$; No D): DVT, patency of major venous systems (portal, vena cava). Carotid Doppler for TIA patient with possible thromboembolic event originating in carotid. Vascular bruit, potential arterial stenosis.

Angiography ($$$; DDD): Aorta, major branches for central and peripheral vascular disease. Abdominal aortic aneurysm, thoracic aortic dissection, major arterial stenosis (renal artery, femoral artery). Vasculitis or mesenteric ischemia. Pre-operative evaluation of aortofemoral bypass.

CTA of aorta and major branches ($$$; DDD): Quick evaluation of trauma when aortic dissection or injury is suspected. Assessment of aneurysm.

Vascular MRI or MRA/MRV ($$$; No D): Aortic aneurysm, relation to other major vessels; take-off of renal arteries; pre-op before aneurysm grafting.

References

1 Patton DD. Insights on the radiologic centennial – a historical perspective. Roentgen and the "new light". I. Roentgen and Lenard. *Invest Radiol* 1992;**27**:408–14.

2 Patton DD. Roentgen and the "new light" – Roentgen's moment of discovery. Part 2: The first glimmer of the "new light". 1993;**28**:51–8.

3 Patton DD. Roentgen and the "new light" – Roentgen's moment of discovery. Part 3: The genealogy of Roentgen's barium platinocyanide screen. 1993;**28**:954–61.

4 Seliger HH. Wilhelm Conrad Röntgen and the glimmer of light. *Phys Today* 1995;Nov:25–31.